

Robust range of auditory periphery development, eye opening, and brain gene expression in Wistar rat pups that experience variation in maternal backgrounds.

Abbreviated title: Auditory system development in rat pups with different maternal experience.

Authors: Jingyun Qiu^{1*}, Preethi Singh^{1*}, Geng Pan^{1*}, Annalisa de Paolis², Frances A. Champagne³, Jia Liu⁴, Luis Cardoso² and Adrián Rodríguez-Contreras^{1,†}.

¹City University of New York, City College, Department of Biology and Center for Discovery and Innovation, New York, NY 10031.

²City University of New York, City College, Department of Biomedical Engineering, New York, NY 10031.

³University of Texas at Austin, Department of Psychology, Austin, TX 78712.

⁴City University of New York, Advanced Science Research Center at the Graduate Center, Neuroscience Initiative, New York, NY 10031.

* These authors had equal contribution

Corresponding author: Adrián Rodríguez-Contreras

Email: arodriguezcontreras@ccny.cuny.edu

Number of pages: 54

Number of figures: 9

Number of tables: 1

Number of words for abstract: 225

Number of words for introduction: 566

Number of words for discussion: 1454

Conflict of interest statement: The authors declare no competing financial interests

27 Acknowledgements: We would like to thank former lab members and students from Macaulay
28 Honors Program Seminar 3 for discussions and help with behavioral scoring. Gene expression
29 data was obtained and processed with help from the CUNY-ASRC Epigenetic Molecular Core
30 facility staff. Supported by NIH grant SC1DC015907 and a CUNY ASRC-seed award.
31
32 Keywords: Maternal care; hearing onset; eye opening; neurotrophins; HIF pathway.

ABSTRACT

The experience of variation in maternal licking and grooming (LG) is considered a critical influence in neurodevelopment related to stress and cognition, but little is known about its relationship to early sensory development. In this study, we used a maternal selection approach to test the hypothesis that differences in LG during the first week of life influence the timing of hearing onset in Wistar rat pups. We performed a range of tests, including auditory brainstem responses (ABR), tracking of eye opening (EO), micro-CT X-ray tomography, and RT-qPCR to monitor neurodevelopmental changes in the female and male progeny of low-LG and high-LG dams. Our results show that variation in maternal LG is not overtly associated with different timing of ABR onset and EO in the progeny. However, the data provide insight on the delay between hearing onset and EO, on key functional and structural properties that define hearing onset at the auditory periphery, and on changes in brain gene expression that include the first evidence that: a) the hypoxia-sensitive gene expression regulatory pathway is regulated in subcortical and cortical auditory brain regions before hearing onset, and b) implicates maternal LG in the BDNF/TrkB pathway in auditory cortex after hearing onset. Altogether, these findings provide a baseline to evaluate how factors that severely disrupt the early maternal environment may affect the expression of robust developmental sensory programs.

50 SIGNIFICANCE STATEMENT

51 Early life experience during sensitive developmental periods can induce long-term effects on the
52 neurobiological development of the offspring. In the present work we tested the hypothesis that
53 variation in maternal licking and grooming (LG) affects the timing of hearing onset in Wistar rat
54 pups. To our surprise the results did not support the hypothesis. Instead, we found a robust range
55 of early and late auditory development that was independent of maternal LG. Nevertheless, the
56 study provides new findings on the delay between hearing onset and eye opening, on key
57 functional and structural properties that define hearing onset at the auditory periphery, and the
58 first evidence that a) the hypoxia sensitive pathway is regulated in the central auditory system
59 during the sensitive period before hearing onset, and b) maternal LG is implicated in the
60 BDNF/TrkB during the sensitive period after hearing onset. These findings provide a baseline to
61 evaluate how factors that severely disrupt the early maternal environment may affect the
62 expression of robust developmental sensory programs.

INTRODUCTION

In several mammalian species, including humans, maternal care is the main source of nutritional, social, and sensory stimulation that is important for survival and has the potential to impact the neurobiological development of the offspring (Curley and Champagne, 2016; González-Mariscal and Melo, 2017). Variation in rat postpartum maternal licking and grooming (LG) has been used as a model to select dams with individual differences in LG behavior and study the developmental re-programming of the offspring's adult stress response (Liu et al., 1997; Francis et al., 1999; Weaver et al., 2004; Hancock et al., 2005; Barha et al., 2007; Menard and Hakvoort, 2007; Parent and Meaney, 2008; Walker et al., 2008; Cameron et al., 2008; Sakhai et al., 2011). However, characterization of the effects of the rearing experiences provided by dams with different LG phenotypes is incomplete, particularly with respect to how maternal LG may affect sensory development of the offspring during sensitive periods of early postnatal development, when various environmental challenges can severely disrupt mother infant interactions, reduce the chances of survival, and cause severe long-term neurobiological deficits in the progeny (Salmaso et al., 2014; Careaga, Murai and Bauman, 2017).

In a previous study, Adise *et al.* (2014) showed that a 15-minute separation followed by return to the biological or a foster mother accelerated auditory periphery development in Wistar rat pups. The effects were stronger when pups were manipulated at postnatal day 5 (P5), and weaker when pups were manipulated at P1 or P9, suggesting that the effects of maternal separation on auditory development were restricted to a sensitive period of postnatal development that occurs one week before the onset of hearing in this species. However, the contributing factors from the maternal environment, such as specific changes in maternal behavior or physiology were not identified.

In the present study, we tested the hypothesis that variation in maternal LG during the first week of life is associated with differences in the timing of hearing onset in Wistar rat pups. This idea is

89 motivated by previous findings that maternal LG is increased in adoptive Wistar rat dams
90 (Maccari et al., 1995), and that massage treatment during the sensitive period before eye opening
91 (EO) accelerates development of visually evoked potentials in Long-Evans rats (Guzzeta et al.,
92 2009). If the frequency of maternal LG influences the timing of hearing onset in the offspring,
93 then pups within a given litter would have an early or late hearing onset that correlates with the
94 LG phenotype of their mother (Figure 1A). To determine the relationship between maternal LG
95 and neurodevelopmental changes in the progeny, we performed tests of auditory brainstem
96 response (ABR), tracking of eye opening (EO), imaging development of the middle ear cavity
97 using micro-CT X-ray tomography, and monitored changes in gene expression in auditory
98 brainstem and primary sensory cortex of pups reared by low-LG or high-LG dams (Figure 1B-
99 D). Contrary to our expectations, the results show that variation in maternal LG is not overtly
100 associated with different timing of ABR onset and EO in the progeny. Nevertheless, the data
101 provide insight on the delay between hearing onset and EO, on key functional and structural
102 properties that define hearing onset at the auditory periphery, and on changes in brain gene
103 expression that include the first evidence that the hypoxia sensitive pathway and the BDNF/TrkB
104 pathway are regulated during sensitive periods that occur before and after hearing onset,
105 respectively, in Wistar rat pups.

106 METHODS

107 *Animal housing and breeding*

108 Experiments were performed in accordance with the Institutional Animal Care and Use
109 Committee of the City College of New York. Rats were kept in a controlled environment at 22°C
110 with an alternating 12 h light and dark cycle (lights were on at 7:00 hrs and off at 19:00 hrs).
111 Water and food were available *ad libitum*. Four maternal selection experiments were performed
112 during the spring and fall seasons of two consecutive years (two experiments per year). For every
113 selection experiment a cohort of 20 male and 40 female Wistar rats at postnatal day 65 was
114 obtained from a commercial supplier (Charles River). Upon arrival, same sex rat pairs were
115 housed in Plexiglas cages and acclimated to the animal care facility for one week. After
116 acclimation, simple randomization with shuffled cage numbers was used to assign single males
117 to a cage with a female pair. Breeding trios were housed together for five days. At the
118 completion of the breeding period males were removed from the study and female pairs were
119 housed together for 14 more days. From 160 females used in the study a total of 137 had
120 successful pregnancies (range of 32 to 36 dams per cohort). Wistar rats have a gestation period
121 of 22 days. Hence, 19 days after mating females were housed individually in Plexiglas cages that
122 were supplied with paper towels as nesting material. Cages were checked for births everyday at
123 9:00 hrs, 12:00 hrs, and 17:00 hrs. On the day of birth (P0), pups were weighted and dams and
124 their litters were placed in clean Plexiglas cages. Females that were not pregnant were removed
125 from the study. Cages were undisturbed during behavioral scoring between P1 and P6, and
126 routine twice per week cage cleaning resumed after behavioral scoring was finished. At P8, dams
127 and their litters were transported to a satellite room for acclimation before testing.

128

129 *Maternal behavior scoring and selection criteria*

130 Methods for scoring maternal behavior and litter selection were adapted from a previous study
131 (Champagne et al., 2003). In brief, five 1-hour maternal behavior observation sessions were

performed daily at 6:00 hrs, 9:00 hrs, 13:00 hrs, 19:00 hrs, and 21:00 hrs between pup ages P1 to P6. Every 1-hour observation consisted of 3 minute-long bins where the following behaviors were scored if observed: no contact with pups, contact with pups, dam is drinking, dam is eating, dam is self-grooming, dam is nest building, dam is licking and grooming (LG) pups in the anogenital or body region, and various levels of arched-back nursing described previously (Champagne et al., 2003). Unless indicated, LG scores in this study represent the frequency of LG in 100 observations per day (60 observations in the light cycle and 40 observations in the dark cycle) expressed as percent LG per day, or as average percent LG obtained from six-day scores. For every cohort, LG histograms were generated and individual dams were selected if their six-day average LG score was 1 SD above (high-LG) or 1 SD below (low-LG) the six-day average LG score of their cohort. Dams and litters that were not selected were removed from the study.

Developmental tracking

Gender, body weight, onset of auditory brainstem responses (ABRs) and eye opening (EO) were tracked. Pup weight was recorded at P0, daily between P10 and P15, and at P21. Pup gender was determined between P10 and P15 using as joint criteria the anogenital distance and the presence or absence of multiple nipples to distinguish between males and females. EO was determined between P10 and P21, and was scored if at least one eyelid was open.

Auditory brainstem response (ABR) tracking

A total of 199 pups from 17 selected litters were used for ABR tracking. These included 81 pups from 7 low-LG litters (36 females and 45 males) and 118 pups from 10 high-LG litters (68 females and 50 males). Low-LG litters had an average of 12 ± 3 pups (mean \pm SD; range 6 to 16 pups; n=7 litters). High-LG litters had an average of 12 ± 3 pups (mean \pm SD; range 6 to 16 pups; n=10 litters). All ABR measurements were done blind to LG group. ABRs were obtained

daily between P10 and P15, and at P21. Anesthesia was induced inside a Plexiglas chamber with 3-5% isoflurane and maintained through a nose cone with 1.5% isoflurane dissolved in medical grade oxygen (gas flow set at 1 L min⁻¹). ABRs were performed inside a double wall sound attenuated room (IAC). Anesthetized pups were placed onto a heating pad set at 37°C to keep them warm throughout the procedure. Subdermal electrodes were placed behind the right ear (reference electrode), at the vertex (active electrode), and at the left shoulder (ground electrode). A calibrated electrostatic Kanetec MB-FX free field speaker was used to deliver click sounds at 40 Hz with intensities ranging from 102 to 2 dB sound pressure level (SPL) in 5 dB decrements. Clicks were synthesized with TDT system 3 hardware (Tucker-Davis Technologies), and presented at 20 kHz with alternating polarity to minimize the presence of stimulus artifacts. Speaker calibration was done with a type 7012 ½ inch ACO Pacific microphone (reference 20 µPa). ABR waveforms were recorded with a Medusa preamplifier at 24.4 kHz and saved to hard disk for offline analysis (Tucker-Davis Technologies). ABRs in this study are average waveforms of 300 traces with 10 ms duration. ABR measurements per litter were completed in 30-40 minutes, including the time it took for pups to recover from anesthesia. After recovery, all pups were placed back into their home cages until the next day of testing.

Combined ABR and micro-CT X-ray tomography (micro-CT) experiments

A total of 56 pups from four litters were used for correlative ABR and micro-CT measurements. These included 27 pups from two low-LG litters (11 females and 14 males) and 29 pups from two high-LG litters (11 females and 18 males) that were obtained from the first and fourth cohorts (one low-LG litter and one high-LG litter from each cohort). On the first day of experiments at P10, pups within a litter were labeled with permanent ink, sexed and processed for ABRs in pairs. After ABRs were measured, anesthetized pups were decapitated and their heads were processed fresh for micro-CT imaging. Micro-CT images were acquired and processed as described previously (Adise et al., 2014). X-Ray projections were generated around

the samples with 0.4° rotation steps at a resolution of 11.5 µm per pixel using a 1172 Bruker SkyScan (Bruker). Scans were loaded into MIMICS (v14.0, Materialise) for segmentation and 3D reconstruction. With the exception of the postalignment compensation, all reconstruction parameters were applied identically to all scans. Micro-CT imaging was performed blind to LG group. This procedure was repeated between P10 and P15 until all pups within a litter were used. For the low-LG and the high-LG litters obtained from the last selection experiment, all pups were screened for ABRs between P10 and P15 and pairs were removed daily for micro-CT imaging. This procedure allowed us to track ABRs between P12 and P13, when major changes in air volume of middle ear cavity and physiological responses were observed.

Gene Expression

The expression of 30 genes implicated in the development and physiology of neuronal, glial and vascular cells in brainstem and cortical brain regions was examined with RT-qPCR in a total of 21 pups from either sex obtained from spring cohorts. We compared 4 developmental stages comprising birth (P0; n=3 pups, each from different litters); the end of the first postnatal week at P7 (n=3 low-LG pups from two litters, and 3 high-LG pups from one litter); the end of the second postnatal week at P15 (n=3 low-LG pups from two litters, and 3 high-LG pups from one litter); and the weaning age at P21 (n=3 low-LG pups, each from different litters, and 3 high-LG pups from two litters).

RT-qPCR was performed with QuantStudio 7 Flex Real-time qPCR system (Thermofisher), using protocols available at the Advanced Science and Research Center Epigenetic Core Facility. Briefly, primer pairs were obtained from a commercial vendor (Sigma-Aldrich) and primer specificity was tested with adult rat whole-brain cDNA. **Table 1** shows the list of primers used in this study in the same order as they appear in **Figures 6, 7 and 8**. Total RNA was isolated from a bank of frozen brains kept at -80 °C using a RNA isolation kit according to the manufacturer's

instructions (Qiagen). Frozen brain samples were thawed and dissected from 5 different regions: cochlear nucleus, pons (ventral brainstem containing the acoustic stria), inferior colliculus, temporal cortex (here referred as auditory cortex), and occipital cortex (here referred as visual cortex). Reverse transcription and specific target amplification were completed using qScript cDNA Supermix (Quanta) according to manufacturer's protocol. A primer mixture containing both forward and reverse primers was mixed with cDNA from different brain regions and loaded onto 384 well plates using an automated PipetMax (Thermofisher). Reverse transcription and specific target amplification were done in a single program. Several cycles of qPCR amplification were performed followed by a melting-curve analysis. The QuantStudio software was used for data analysis and visualization. Threshold was determined automatically and Ct values were calculated using QuantStudio software. The housekeeping gene β -actin was measured for all ages and LG conditions tested using primers described in **Table 1**.

Data Analysis

ABR recordings were saved as text files and analyzed using NeuroMatic in Igor Pro software (WaveMetrics; Rothman and Silver, 2018). ABR thresholds were determined using an amplitude criterion to detect responses that were larger than four times the standard deviation (SD) of the baseline (Bogaerts et al., 2009). In general, waveforms with amplitudes larger than 1 microvolt were considered auditory responses. Wave I was defined as a positive transient voltage change with a peak latency of 1.8 ms to 2.2 ms. Short latency potentials (SLPs) were defined as positive transient voltage changes with a peak latency ~ 1 ms.

Developmental curves of percent pups with a wave I response, EO, or air volume at different ages were fit to **Equation 1**:

$$Y = Y_0 + (Y_{\max} - Y_0) / [1 + \exp(A_{50} - X/k)] \quad (1)$$

236

237 Where Y_0 is the minimum observed Y (i.e., the percent pups with ABR, EO, or air volume),
238 Y_{max} is the maximum observed Y, A_{50} is the age at which Y is half maximum, X is age (in
239 days), and k is the rate coefficient.

240

241 *Statistics*

242 Unless indicated, data represent mean \pm SD. Statistical analyses were done with Prism 6 software
243 (GraphPad). When appropriate, data sets were tested for normality using the D'Agostino and
244 Pearson omnibus K2 test. Means in **Figure 2** were compared with an ordinary one-way ANOVA
245 and the Holm-Sidak's multiple comparisons test (**Figure 2A**), or the Tukey's multiple
246 comparisons test (**Figure 2D**). Medians in **Figure 3** were compared with the ANOVA Kruskal-
247 Wallis test and the Dunn's multiple comparisons test (**Figure 3E and F**). Gene expression data
248 was analyzed by ANOVA Kruskal-Wallis test and the Dunn's multiple comparisons test. Alpha
249 = 0.05 was used to denote significance when testing for statistical differences between means or
250 medians.

RESULTS

Variation in maternal LG

We used four Wistar rat cohorts from the spring and summer seasons of two consecutive years to select low-LG and high-LG dams, and we tracked the sensory development of their pup's between postnatal ages P10 and P21 (**Figure 1B**). **Figure 2A** shows box plots of maternal LG scores from the four cohorts used in this study. The six-day average LG score for each cohort was (mean \pm SD): 9.8 ± 1.8 (n=36 dams, spring year 1); 7.7 ± 2.2 (n=33 dams, summer year 1); 11.2 ± 1.6 (n=36 dams, spring year 2); and 7.9 ± 1.9 (n=32 dams, summer year 2). Statistical analysis showed significant differences between mean LG scores (Ordinary one-way ANOVA, $F=25.91$, $P<0.0001$), in particular between spring cohorts, and between spring and summer cohorts. Mean summer cohort LG scores were not significantly different from each other (determined by Tukey's multiple comparisons test; see **Figure 2** legend for P values). The large variability in LG scores across cohorts prompted us to examine the daily LG scores of the seven low-LG dams and the ten high-LG dams that were selected. Low-LG dams selected from spring cohorts showed daily LG profiles that started high and decreased during the six-day observation period (continuous lines in **Figure 2B**), while low-LG dams selected from summer cohorts showed relatively lower LG scores throughout the six-day observation period (dashed lines in **Figure 2B**). High-LG dams had daily LG scores that were very variable but stayed relatively high throughout the six-day observation period, regardless of whether they were obtained from the spring or summer cohorts (**Figure 2C**). Statistical analysis showed significant differences between the six-day average LG scores of selected dams (**Figure 2D**; ordinary one-way ANOVA, $F=31.93$, $P<0.0001$). We found that the average LG score of low-LG dams was higher in spring cohorts compared to summer cohorts (Tukey's multiple comparisons test, $P=0.0035$). In contrast, we did not find statistically significant differences between the six-day average LG scores of high-LG dams from spring and summer cohorts (Tukey's multiple comparisons test,

P=0.5672). Overall, these results show that despite the variable LG scores between cohorts, the LG scores of selected low-LG and high-LG groups were significantly different from each other.

Variation in auditory brainstem response (ABR) onset and eye opening (EO) in pups reared by low-LG and high-LG dams

ABRs and EO were tracked in a total of 81 pups from seven low-LG litters and in 118 pups from ten high-LG litters. For each litter the percent of pups with an ABR wave I, or the percent of pups with EO were plotted at different ages, and fits to **Equation 1** were obtained (**Figure 3A, B, C and D**; continuous lines represent fits to data from spring litters, dashed lines represent fits to data from summer litters). To examine the variation in ABR onset and EO within and across LG groups, the distributions of A_{50} values were compared (**Figure 3E**). This qualitative analysis showed skewed ABR A_{50} distributions for low-LG and high-LG litters, indicating that the majority of pups examined had early ABR onset between P11.5-P12. However, in some litters pups had ABR onset as late as P13-P13.5. EO A_{50} distributions for low-LG and high-LG litters were also skewed and covered a range of two days between P13 and P15. Statistical analysis showed significant differences between A_{50} medians (Kruskal-Wallis test, P value <0.0001). A more detailed examination showed that the ABR A_{50} medians between low-LG and high-LG litters were not significantly different from each other (Dunn's multiple comparisons test, see **Figure 3** legend for P values). A similar result was obtained for EO A_{50} medians (Dunn's multiple comparisons test, see **Figure 3** legend for P values). However, the ABR A_{50} medians were significantly different from the EO A_{50} medians, within and across LG groups (indicated by asterisks in **Figure 3E**; Dunn's multiple comparisons test, see **Figure 3** legend for P values). To obtain information on the synchrony of development within litters, ABR and EO rate coefficient k distributions were compared (see **Equation 1** and **Figure 3F**). The data shows evidence of predominately short values of rate coefficient k for low-LG and high-LG litters. Neither ABR rate coefficient k medians nor EO rate coefficient k medians showed significant differences

within and across LG groups (Kruskal-Wallis test, P value=0.1171). In sum, experiments described in **Figures 1B, 2, and 3** show that despite significant differences in LG scores between selected dams, ABR onset, timing of EO and synchrony of development do not differ between low-LG and high-LG litters. Instead, there is a range of litter-specific early or late times for ABR onset that happens during a two-day period. Similarly, a two-day range for early and late EO takes place sequentially after ABR onset.

Maternal LG is not correlated with ABR onset or EO

We used scatter plots of ABR A_{50} or EO A_{50} values against LG scores to determine the correlation coefficients between these two variables. We did not find evidence of a correlation between ABR A_{50} values and LG scores (non parametric Spearman correlation, $R=-0.1063$, two-tailed $P=0.6823$), or between EO A_{50} values and LG scores (non parametric Spearman correlation $R=-0.05184$, two-tailed $P=0.8434$). We also checked for systematic differences in the growth of pups reared by low-LG and high-LG dams. We compared average pup body weight between females and males within a litter and across LG groups on the day of ABR onset (defined by the A_{50} parameter) or using the slope of the growth curve between P10 and P15 (determined by linear regression of body weight data). This analysis showed that pup's body weight did not correlate with maternal LG scores. Similar results were obtained when we tested for developmental differences between male and female pups (data not shown). Overall, the data discussed in this section does not support a correlation between maternal LG scores and developmentally tracked features of male and female pups.

Differences in the delay between ABR onset and EO in litters with early or late ABR onset

Next, we examined ABR onset and EO data in scatter plots of EO A_{50} values plotted against ABR A_{50} values (**Figure 4A**). This analysis showed that in individual litters, ABR onset always happened before EO, and notably, it confirmed that for both, ABR and EO, there was a range of

early and late onset times that happened within a two-day window: while ABR onset was observed between P11.5 and P13.5, EO was observed between P13 and P15. Note that there was never a litter in which the age of EO coincided with the age of ABR onset. Instead, litters with the earliest ABR onset had more variable EO times than litters with late ABR onset. In litters with ABR onset around P11.5 and P12, we observed delays to EO from 1.5-days to 3.5-days. In contrast, in litters with late ABR onset at ~P13, there was a ~1.5-2 day delay to EO. This pattern was observed in low-LG and high-LG litters alike (**Figure 4A**). A similar comparison between EO and ABR rate coefficient k showed that in most litters ABR rate coefficient values were <0.1 , implying developmental synchrony within litters. In contrast, EO rate coefficients were more variable, implying developmental synchrony and asynchrony, respectively across different litters (**Figure 4B**).

Relationship between the development of the middle ear and ABR thresholds in the progeny of low-LG and high-LG dams

To obtain information about developmental structural changes in the auditory periphery of pups from low-LG and high-LG litters, four litters were used to perform correlative ABR and micro CT X-ray tomography (micro-CT) experiments (**Figure 1C**; $n=51$ pups). Detailed examination of the 3D renderings generated from micro-CT data confirmed our previous finding that formation of the middle ear cavity precedes formation of the ear canal (**Figure 5A**; Adise et al., 2014). However, in contrast to previous studies, precursor zones or small air pockets were not observed. Instead, there were marked differences in the air volume of pups from different litters, particularly between P12 and P13 (**Figure 5B**). Fitting **Equation 1** to data in **Figure 5B** gave A_{50} values that ranged from 11.8 days to 13.2 days (12.4 ± 0.3 days, $n = 4$ litters), and rate coefficient k values that ranged from 0.28 to 0.47 (0.40 ± 0.04 , $n = 4$ litters). From the 51 pups used in micro-CT imaging experiments, we confirmed an ABR wave I in 25 pups between P12 and P15, while 17 pups between ages P10 and P11, and 9 pups between ages P12 and P13 did

not show any evidence of ABR wave I (**Figure 5C**). Since the micro-CT imaging did not detect air in any of the 17 non-responsive (NR) pups examined between P10 and P11, we can infer that formation of an air-filled middle ear cavity is necessary for transmission of airborne pressure waves to the inner ear. Linear fitting of wave I threshold data versus air volume in the range between 25 mm³ to 60 mm³ gave a slope of -2.5 dB/mm³, showing that auditory thresholds are inversely proportional to air volume in the auditory periphery. However, the structural data also suggests that the presence of air in the middle ear may not be sufficient for proper sound transmission, since there were 7 animals with a measurable air volume in the middle ear at P12 and P13 that did not show an ABR wave I (labeled non responsive, NR, in the boxed area of **Figure 5C**).

To examine the possibility that a minimal air volume at the auditory periphery is necessary for the onset of ABRs, the ABR waveforms from all pups at P12 (n=10) and all pups at P13 (n=8) used in the combined ABR and micro-CT experiments were re-examined. To our surprise, seven P12 pups and six P13 pups with air volumes larger than 12 mm³ had responses of comparable amplitude to wave I, but with a shorter latency. We refer to these events as short latency potentials (SLPs; **Figure 6**). **Figure 6D** shows exemplar ABR traces with SLPs at different click intensities in a P12 pup whose structural information is shown in **Figure 6C**. Note that in this example wave I was not present, determined by the absence of a positive potential with a latency ~2 ms. **Figure 6F** shows exemplar recordings from another P12 pup that had SLPs followed by wave I at different click intensities and whose structural data is shown in **Figure 6E**. Note that in this example a wave I was identified after the SLP at click intensities of 102 dB and 97 dB but not at lower intensities, demonstrating that the threshold for the SLP was lower than the threshold for wave I. Lastly, exemplar ABR traces are shown for a P12 pup with an air volume of zero in the middle ear. In this case SLPs and wave I were absent in response to the same click intensities probed for the other pups (**Figure 6A and B**). Based on these observations, we re-

examined all the ABR recordings from the 4 litters used in combined ABR and micro-CT experiments between P11 and P15 to corroborate the presence or absence of SLPs at different ages. We found evidence of SLPs at P12 ($n = 7$ pups) and P13 ($n = 6$ pups), but we did not find any evidence of SLPs at P11 ($n = 8$ pups), P14 ($n = 8$ pups) and P15 ($n = 8$ pups). **Figure 6G** plots the SLP thresholds as a function of air volume for all ten P12 and eight P13 pups used in the combined ABR and micro-CT experiments (**Figure 6G**, solid symbols). Note that there were four NR P12 pups whose air volumes were $< 15 \text{ mm}^3$ and did not have SLPs or ABR wave I, and one P13 NR pup with an air volume of 34 mm^3 that did not have a SLP but had an ABR wave I (P12 NR pups are enclosed together in a dashed box, and the P13 NR pup with wave I but without SLP is enclosed in a dashed box marked with an arrow in **Figure 6G**). Linear fitting of SLP threshold data versus air volume in the range between 15 mm^3 to 50 mm^3 gave a slope of -0.3 dB/mm^3 . Altogether, these data support the view that a minimal air volume at the auditory periphery is necessary for airborne conduction of click sounds from the external ear to the inner ear. Next, we examined the relationship between SLPs and wave I responses.

SLPs show hallmarks of sensory responses from the inner ear

We hypothesized that SLPs may represent electrical responses in hair cells of the inner ear. Alternatively, SLPs could represent evoked potentials from a different sensory modality, such as somatosensory fibers activated by the pressure energy contained in click stimuli of high intensity. If SLPs were generated in hair cells of the inner ear, then we would expect that SLPs and wave I would show hallmarks of synaptic communication, including a defined delay between events. In addition, we would expect developmental changes in the thresholds and the delay between SLPs and wave I. We would not expect to see these hallmarks if SLPs were sensory responses independent from wave I. To test these predictions, we took advantage that six littermates from one low-LG litter and six littermates from another high-LG litter were not used for micro-CT scans at P12. We recorded ABRs and defined the co-occurrence of SLPs and wave

I, and examined how the threshold for SLPs changed with respect to the threshold of wave I between P12 and P13. We found that all six pups from the high-LG litter had SLPs but did not have a wave I (open blue triangles in **Figure 6H**). Interesting to us, five out of six pups from the low-LG litter had SLPs followed by a wave I, and one pup had SLPs without any evidence of wave I (open magenta triangles in **Figure 6H**). Counting all the pups used in combined ABR and micro-CT experiments and the subset of littermates used in ABR tracking we found that in low-LG litters at P12 there were 2 pups that did not have a SLP nor a wave I (**Figure 6H** box 2); 1 pup had SLPs but not a wave I; 6 pups had SLPs with thresholds that were lower than their corresponding wave I thresholds; and 1 pup had SLPs with a threshold that was similar to its wave I threshold. In high-LG litters at P12 there was 1 pup without SLP and wave I; 10 pups had SLPs and no wave I (**Figure 6H** box 1); and 1 pup had SLPs with a threshold lower than its wave I threshold. Thus, based on this data, it seems that SLPs occur alone at P12, and when SLPs and wave I are observed together, SLPs have lower thresholds than wave I. In low-LG litters at P13, there were 3 pups that had SLPs with thresholds that were lower than wave I thresholds. In high-LG litters at P13, all 3 pups had SLPs with thresholds that were similar to their corresponding wave I thresholds. Thus, at P13, SLPs always co-occur with wave I and had higher or similar thresholds than wave I.

To examine the development of SLPs and wave I responses, we tracked the ABRs from P12 to P13 in the eight remaining littermates from the low-LG and high-LG litters (4 pups per litter). We found evidence of a decrease in wave I thresholds from P12 to P13 such that in 7 of 8 pups SLPs had thresholds that were similar to their corresponding wave I thresholds, and in one pup the wave I threshold was lower than its corresponding SLP threshold (asterisks in **Figure 6H**). This single observation raised the possibility that in this animal, SLPs were independent events of wave I events. To test the possibility that somatosensory fibers could be activated by the pressure wave energy of high intensity click stimuli, we injected the local anesthetic lidocaine

around the skin pad surrounding the pinna area in three P13 littermates used for ABR
 experiments. This manipulation did not affect the occurrence of SLPs in these animals,
 suggesting that skin stimulation by high intensity clicks does not generate SLPs (data not
 shown). Altogether, these results indicate that SLPs antecede the developmental expression of
 wave I responses (open symbols in **Figure 6H**) and suggest that as pups mature, wave I
 thresholds decrease to match SLP thresholds.

Lastly, we obtained estimates of two physiological parameters of SLPs: the latency of events
 from stimulus onset, and the delay between the peaks of SLP's and wave I events at P12 and
 P13. The latency from stimulus onset was evaluated from ABR traces at different intensities
 ranging between 77 dB and 102 dB. We did not find systematic changes in this parameter as a
 function of click intensity at P12 or P13, so we obtained an average SLP latency per pup from
 these combined measurements and obtained a grand average per LG group per age. At P12, the
 latency of SLPs was 1.08 ± 0.01 ms in low-LG pups (n=8 pups) and 1.09 ± 0.01 ms in high-LG
 pups (n=11 pups). At P13, the latency of SLPs was 1.09 ± 0.01 ms in low-LG pups (n=7 pups)
 and 1.07 ± 0.01 ms in high-LG pups (n=7 pups). The mean values of SLP latency for different
 LG groups and ages were not significantly different from each other (age $P=0.6342$; LG group
 $P=0.6342$; interaction between age and LG group $P=0.1598$, 2 way ANOVA). At P12, the delay
 between the peaks of the SLP and wave I was 1.01 ± 0.03 ms in low-LG pups (n=7 pups), and
 could not be determined in high-LG pups since they did not have a wave I at this age, or if they
 had a wave I it was not preceded by a SLP (boxed data point indicated with an arrow in **Figure**
6G and H). At P13, the delay between the peaks of the SLP and wave I was 1.03 ± 0.03 ms in
 low-LG pups (n=7 pups), and 1.02 ± 0.02 ms in high-LG pups (n=7 pups). Altogether, data in
Figures 5 and 6 show the relationship between development of the auditory periphery and the
 type of sensorineural response recorded in the progeny of low-LG and high-LG pups. SLPs

predominated over wave I responses at P12, and gradually waned as wave I responses increased in amplitude at P13 and thereafter.

Analysis of gene expression in the auditory brainstem, auditory cortex (ACX) and visual cortex (VCX) of pups reared by low-LG and high-LG dams

A gene expression screen using RT-qPCR was carried out with pup tissue from five brain regions at four ages. We screened the relative mRNA expression levels of 30 genes involved in neuronal, glial and vascular physiology and development in samples from the cochlear nucleus (CN), the pons, the inferior colliculus (IC), the primary auditory cortex (ACX), and the primary visual cortex (VCX) from neonate pups at P0, P7, P15, and P21 (Figure 1C; n=3 pups per age per LG group). Gene expression data is expressed as fold change with respect to P0 and summarized in **Figures 7, 8 and 9**.

Analysis of genes involved in developmental plasticity

Figure 7 shows results for 10 genes involved in developmental plasticity, including transcriptional regulation and signal transduction. **Figure 7A** shows expression profiles for the neurotrophins BDNF and NGF, and for the BDNF receptor TrkB. The relative levels of BDNF mRNA in subcortical structures did not change between P0 and any other age examined (ordinary one-way ANOVA $P=0.5135$, $P=0.5157$, $P=0.2458$, for CN, pons, and IC, respectively). For cortical structures, there was a statistically significant increase in ACX and VCX of high-LG pups between P0 and P21 (ordinary one-way ANOVA $P=0.0730$, $P=0.0175$, for ACX and VCX, respectively; and multiple comparisons test $P=0.0192$ and $P=0.0035$, for ACX and VCX respectively). The relative levels of NGF mRNA did not show statistically significant changes in subcortical structures between P0 and any other age examined (ordinary one-way ANOVA $P=0.4500$, $P=0.4226$, $P=0.3039$ for CN, pons and IC, respectively). However, NGF mRNA levels showed a statistically significant increase in ACX and VCX of pups from both LG groups

between P0 and P21 (ordinary one-way ANOVA $P=0.0001$ and $P=0.0001$, for ACX and VCX respectively; and multiple comparisons test $P=0.0001$, $P=0.0007$, for low-LG and high-LG samples in ACX respectively; $P=0.0001$, $P=0.0007$, for low-LG and high-LG samples in VCX, respectively). Similar to BDNF and NGF mRNAs, TrkB mRNA levels did not show changes in CN and pons between P0 and any other age examined (ordinary one-way ANOVA $P=0.5272$ and $P=0.523$ for CN and pons, respectively). However, there was a significant increase of TrkB mRNA levels in the IC of high-LG pups between P0 and P15, and a significant increase of TrkB mRNA levels in the IC of low-LG pups between P0 and P21 (ordinary one-way ANOVA $P=0.0324$; and multiple comparisons test $P=0.0024$, $P=0.0040$ for high-LG samples at P15 and low-LG samples at P21, respectively). TrkB mRNA levels showed statistically significant increases in ACX and VCX of low-LG and high-LG pups between P0 and P15, and between P0 and P21 (ordinary one-way ANOVA $P=0.0004$ and $P=0.0023$ for ACX and VCX, respectively; multiple comparisons $P=0.0003$, $P=0.0056$, for low-LG and high-LG samples in ACX, respectively; $P=0.0056$, $P=0.0001$, for low-LG and high-LG samples in VCX, respectively). It was noted that the relative levels of TrkB mRNA in the ACX were significantly different between low-LG and high-LG samples at P21 (boxed region in ACX TrkB panel of **Figure 7A**; multiple comparisons test $P=0.0437$).

Figure 7B shows developmental expression profiles for transcription factors c-Fos, c-Jun, NfκB, and Otx2. In the auditory brainstem the relative level of expression of c-Fos mRNA showed a small increase in CN of low-LG and high-LG pups between P0 and P21 (one-way ANOVA $P=0.0032$; and multiple comparisons test $P=0.0065$, $P=0.0021$ for low-LG and high-LG samples, respectively). No significant changes in c-Fos mRNA were detected in pons between P0 and any other age examined (one-way ANOVA $P=0.2129$), while there was an increase in c-Fos mRNA in the IC of high-LG pups between P0 and P21 (one-way ANOVA $P=0.0426$; and multiple comparisons test $P=0.0115$). In contrast, c-Fos mRNA levels showed robust increases in

509 ACX of pups from both LG groups between P0 and P15 (one-way ANOVA $P=0.0148$; and
510 multiple comparisons test $P=0.0060$, $P=0.0485$, for low-LG and high-LG samples, respectively),
511 and between P0 and P21 (multiple comparisons test $P=0.0201$, $P=0.0360$, for low-LG and high-
512 LG samples, respectively). c-Fos mRNA levels increased in VCX of low-LG pups between P0
513 and P15 (one-way ANOVA $P=0.0076$; multiple comparisons $P=0.0411$), and in low-LG and
514 high-LG pups between P0 and P21 (multiple comparisons test $P=0.0029$, $P=0.0119$, for low-LG
515 and high-LG samples, respectively). In the auditory brainstem, the relative level of expression of
516 c-Jun mRNA showed an increase in the CN and IC of low-LG and high-LG pups between P0
517 and P21 (one-way ANOVA $P=0.0022$, $P=0.0002$ for CN and IC, respectively; and multiple
518 comparisons test $P=0.0060$, $P=0.0002$ for low-LG and high-LG CN samples, respectively; and
519 $P=0.0001$, $P=0.0012$ for low-LG and high-LG IC samples, respectively). In the pons, c- Jun
520 mRNA levels increased in low-LG pups between P0 and P15 (one-way ANOVA $P=0.0001$; and
521 multiple comparisons test $P=0.0246$), and in both LG groups between P0 and P21 (multiple
522 comparisons test $P=0.0001$, $P=0.0001$ for low-LG and high-LG pons samples, respectively). c-
523 Jun mRNA levels showed significant increases in the ACX of pups from both LG groups
524 between P0 and P15 (one-way ANOVA $P=0.0001$; and multiple comparisons test $P=0.0106$,
525 $P=0.0030$, for low-LG and high-LG samples, respectively), and between P0 and P21 (multiple
526 comparisons test $P=0.0001$, $P=0.0001$, for low-LG and high-LG samples, respectively). c-Jun
527 mRNA levels increased in VCX of low-LG pups between P0 and P15 (one-way ANOVA
528 $P=0.0101$; multiple comparisons $P=0.0158$), and in low-LG and high-LG pups between P0 and
529 P21 (multiple comparisons test $P=0.0032$, $P=0.0079$, for low-LG and high-LG samples,
530 respectively). The relative expression of NfκB mRNA did not change during development in the
531 CN and pons (one-way ANOVA $P=0.3487$, $P=0.3995$, for CN and pons, respectively). In the IC,
532 NfκB mRNA levels showed a slight but significant decrease in high-LG pups between P0 and P7
533 (one-way ANOVA $P=0.0001$; multiple comparisons test $P=0.0100$), and an increase in low-LG

pups between P0 and P21 (multiple comparisons $P=0.0001$). The profile of NfκB mRNA expression was similar in the ACX and VCX, where there was an increase in low-LG pups between P0 and P15 (one-way ANOVA $P=0.0001$ and $P=0.0001$ for ACX and VCX, respectively; multiple comparisons test $P=0.0157$, $P=0.0003$ for low-LG samples in ACX or VCX, respectively), and an increase in pups from both LG groups between P0 and P21 (multiple comparisons test $P=0.0001$, $P=0.0001$, for low-LG and high-LG in ACX, respectively; and $P=0.0001$, $P=0.0001$, for low-LG and high-LG in VCX, respectively). It was noted that the relative levels of NFκB mRNA in the ACX were significantly different between low-LG and high-LG samples at P21 (boxed region in ACX NFκB panel of **Figure 6B**; multiple comparisons test $P=0.0002$). Lastly, the relative levels of expression of Otx2 mRNA did not change during development in any of the brain structures examined (multiple comparisons test; $P=0.4064$, $P=0.7841$, $P=0.4302$, $P=0.2075$, $P=0.4808$, for CN, pons, IC, ACX and VCX, respectively).

Figure 7C shows mRNA developmental expression profiles for three downstream signaling effectors: the kinases Akt1 and Akt2, and Sort1, a protein involved in the transport of other proteins from intracellular membrane compartments to the plasma membrane. In the CN, the relative levels of expression of Akt1 increased between P0 and P15 in high-LG pups (one-way ANOVA $P=0.0107$; multiple comparisons test $P=0.0003$). It was noted that the relative level of Akt1 mRNA was significantly different between low-LG and high-LG groups at P15 (boxed region in CN Akt1 panel in **Figure 7C**; multiple comparisons test $P=0.0030$). In the CN, Akt1 mRNA levels increased between P0 and P21 in both LG groups (multiple comparisons test $P=0.0252$, $P=0.0101$ for low-LG and high-LG samples, respectively). The levels of Akt1 mRNA did not change during development in pons, IC, ACX and VCX (one-way ANOVA $P=0.589$, $P=0.71611$, $P=0.2611$ and $P=0.1680$ for pons, IC, ACX and VCX, respectively). In contrast to Akt1 mRNA levels, the relative levels of Akt2 mRNA increased in the CN, IC and VCX

between P0 and P21 in both LG groups (one-way ANOVA $P=0.0121$, $P=0.0012$, $P=0.0026$ for CN, IC and VCX, respectively; multiple comparisons $P=0.0020$, $P=0.0055$ for low-LG and high-LG samples in CN; $P=0.0004$, $P=0.0015$, for low-LG and high-LG samples in IC; $P=0.0457$, $P=0.0049$, for low-LG and high-LG samples in VCX, respectively). In the pons, Akt2 mRNA levels did not change between P0 and any age examined (one-way ANOVA $P=0.6949$). In the ACX, Akt2 mRNA levels increased in high-LG pups between P0 and P15 (one-way ANOVA $P=0.0001$; multiple comparisons test $P=0.0143$), and in both LG groups between P0 and P21 (multiple comparisons test $P=0.0001$, $P=0.0001$, for low-LG and high-LG groups, respectively). Lastly, the levels of Sort1 mRNA in the CN, ACX and VCX showed increased levels in both LG groups between P0 and P15 (one-way ANOVA $P=0.0001$, $P=0.0001$, $P=0.0001$, for CN, ACX and VCX, respectively; multiple comparisons test $P=0.0321$, $P=0.0187$ for low-LG and high-LG samples in CN, respectively; $P=0.0050$, $P=0.0059$ for low-LG and high-LG samples in ACX, respectively; and $P=0.0017$, $P=0.0138$, for low-LG and high-LG samples in VCX, respectively), and between P0 and P21 (multiple comparisons test $P=0.0001$, $P=0.0001$, for low-LG and high-LG samples in CN, respectively; $P=0.0001$, $P=0.0001$, for low-LG and high-LG samples in ACX, respectively; and $P=0.0001$, $P=0.0001$, for low-LG and high-LG samples in VCX, respectively). In the pons and IC, the levels of Sort1 mRNA increased in both LG groups between P0 and P21 (multiple comparisons test $P=0.0001$, $P<0.0001$, for low-LG and high-LG samples in pons, respectively; and $P=0.0224$, $P=0.0002$, for low and high-LG samples in IC, respectively). It was noted that mRNA levels in IC were statistically different between low-LG and high-LG samples at P21 (multiple comparisons test $P=0.0329$).

In sum, the data in **Figure 7** shows evidence that genes involved in transcriptional regulation and signal transduction the context of developmental plasticity, increased expression levels in the ACX and VCX between P0 and P21, and to some extent between P0 and P15. Similar age-dependent expression profiles were observed in the CN and IC, but not consistently in the pons.

Statistically significant differences between samples from pups of low-LG and high-LG litters were observed in the ACX at P21 (TrkB and NFkB), in the CN at P15 (Akt1), and in the IC at P21 (Sort1).

Analysis of genes involved in myelin development, the hypoxia-sensitive pathway and the Wnt pathway

Figure 8 shows results for 10 genes that are involved in myelin development and two distinct signaling pathways. **Figure 8A** shows developmental expression profiles for Olig2 and Mbp. In the CN, the relative levels of Olig2 mRNA showed a significant increase in low-LG and high-LG samples between P0 and P21 (one-way ANOVA $P=0.0250$; multiple comparisons test $P=0.0066$, $P=0.0067$, for low-LG and high-LG samples, respectively), but there were no significant differences observed in the pons, IC, ACX and VCX between P0 and any age tested (one-way ANOVA, $P=0.4959$, $P=0.7710$, $P=0.5170$, $P=0.3840$, for pons, IC, ACX and VCX, respectively). The relative levels of Mbp mRNA showed an increase in the CN of low-LG pups between P0 and P21 (one-way ANOVA $P=0.0068$; multiple comparisons test $P=0.0415$). In the pons, Mbp mRNA levels decreased significantly in low-LG pups between P0 and P15 (one-way ANOVA $P=0.3076$; multiple comparisons test $P=0.0238$). In the IC, Mbp mRNA levels increased in high-LG pups between P0 and P21 (one-way ANOVA $P=0.0073$; multiple comparisons test $P=0.0037$). In ACX and VCX, Mbp mRNA levels increased in low-LG and high-LG pups between P0 and P21 (one-way ANOVA $P=0.0002$, $P=0.0001$ for ACX and VCX, respectively; multiple comparisons test $P=0.0003$, $P=0.0004$, for low-LG and high LG samples in ACX, respectively; $P=0.0001$, $P=0.0002$, for low-LG and high LG samples in VCX, respectively).

Figure 8B shows developmental expression profiles for hypoxia-sensitive transcription factors Hif1a and Hif2a, and for their regulator Phd isoforms 1-3. In the CN, IC and VCX, the relative levels of Hif1a mRNA did not change between P0 and any age examined (one-way ANOVA

611 P=0.4775, P=0.3494, P=0.0716 for CN, IC and VCX, respectively). In the pons and ACX, a
 612 significant increase in Hif1a mRNA levels was detected in high-LG pups between P0 and P21
 613 (one-way ANOVA P=0.1645, P=0.0699 for pons and ACX, respectively; multiple comparisons
 614 test P=0.0171, P=0.0203 for high-LG samples in pons and VCX, respectively). In the CN, pons,
 615 IC, ACX and VCX, the relative levels of Hif2a mRNA showed increases between P0 and P15
 616 and between P0 and P21 (one-way ANOVA P=0.0165, P=0.0303, P=0.00174, P=0.0001,
 617 P=0.0001 for CN, pons, IC, ACX and VCX, respectively). In the CN, an increase in Hif2a
 618 mRNA in high-LG pups was observed between P0 and P15, while in the IC, an increase in low-
 619 LG pups between P0 and P15 was detected (multiple comparisons test P=0.0237, P=0.0092 for
 620 CN and IC, respectively). In the CN and IC, there was an increase of Hif2a mRNA in both LG
 621 groups between P0 and P21 (multiple comparisons test P=0.0154, P=0.0119 for low-LG and
 622 high-LG samples in CN, respectively; P=0.0400, P=0.0021 for low-LG and high-LG samples in
 623 IC, respectively). In the pons, ACX, and VCX, an increase in Hif2a mRNA was observed in both
 624 LG groups between P0 and P15 (multiple comparisons test P=0.0147, P=0.0105 for low-LG and
 625 high-LG pups in pons, respectively; P=0.0500, P=0.0104 for low-LG and high-LG pups in ACX,
 626 respectively; P=0.0006, P=0.0006 for low-LG and high-LG pups in VCX, respectively) and
 627 between P0 and P21 (multiple comparisons test P=0.0011, P=0.0003 for low-LG and high-LG
 628 pups in pons, respectively; P=0.0001, P=0.0001 for low-LG and high-LG pups in ACX,
 629 respectively; P=0.0002, P=0.0001 for low-LG and high-LG pups in VCX, respectively). The
 630 developmental expression profile of Phd1 mRNA was heterogeneous. In the CN, there was a
 631 significant increase in low-LG and high-LG groups between P0 and P21 (one-way ANOVA
 632 P=0.1932; multiple comparisons test P=0.0303, P=0.0479 for low-LG and high-LG pups,
 633 respectively). In the pons and IC, there were no changes detected in Phd1 mRNA levels between
 634 P0 and any age examined (one-way ANOVA P=0.9052, P=0.9349 for pons and IC,
 635 respectively). In the ACX, there were increases in Phd1 mRNA of high-LG pups between P0 and
 636 P7 (one-way ANOVA P=0.0976, multiple comparisons test P=0.0351), and in both LG groups

637 between P0 and P15 (multiple comparisons test $P=0.0202$, $P=0.0096$). In the VCX, there were
 638 increases in Phd1 mRNA in both LG groups between P0 and P15 (one-way ANOVA $P=0.0599$;
 639 multiple comparisons test $P=0.0205$, $P=0.0055$). The developmental expression profile of Phd2
 640 mRNA levels was the first to show consistent changes between P0 and P7 across different brain
 641 regions. In the CN and ACX, there were decreases in Phd2 mRNA levels in both LG groups
 642 between P0 and P7 (One-way ANOVA $P=0.0001$, $P=0.0001$; multiple comparisons test
 643 $P=0.0050$, $P=0.0240$, for low and high-LG samples in CN; $P=0.0163$, $P=0.0066$ for low-LG and
 644 high-LG samples in ACX), and in both LG groups between P0 and P15 (multiple comparisons
 645 test $P=0.0084$, $P=0.0098$ for low-LG and high-LG samples in CN; $P=0.0119$, $P=0.0080$ for low-
 646 LG and high-LG samples in ACX). In the CN and ACX, there were increases in Phd2 mRNA
 647 levels in both LG groups between P0 and P21 (multiple comparisons test $P=0.0156$, $P=0.0078$
 648 for low-LG and high-LG samples in CN; $P=0.0001$, $P=0.0001$ for low-LG and high-LG samples
 649 in ACX). In the pons, there was a decrease in Phd2 mRNA levels in low-LG samples between P0
 650 and P7 (one-way ANOVA $P=0.0262$; multiple comparisons test $P=0.0452$). In the IC, there were
 651 decreases in Phd2 mRNA levels in both LG groups between P0 and P7 (one-way ANOVA
 652 $P=0.0001$; multiple comparisons test $P=0.0267$, $P=0.0357$), in high-LG pups between P0 and P15
 653 (multiple comparisons $P=0.0334$), and increases in both LG groups between P0 and P21
 654 (multiple comparisons $P=0.0004$, $P=0.0005$ for low-LG and high-LG samples respectively).
 655 Lastly, in the VCX there were increases in Phd2 mRNA levels in both LG groups only between
 656 P0 and P21 (one-way ANOVA $P=0.0001$; multiple comparisons test $P=0.0009$, $P=0.0007$ for
 657 low-LG and high-LG samples, respectively). The developmental expression profile of Phd3
 658 mRNA in the CN, pons, and VCX, showed increases in both LG groups between P0 and P21
 659 (one-way ANOVA $P=0.0001$, $P=0.0001$, $P=0.0003$ in CN, pons and VCX, respectively; multiple
 660 comparisons test $P=0.0008$, $P=0.0001$ for low-LG and high-LG samples in CN, respectively;
 661 $P=0.0009$, $P=0.0001$ for low-LG and high-LG samples in pons, respectively; $P=0.0016$,
 662 $P=0.0020$ for low-LG and high-LG samples in VCX, respectively). In the IC, there were no

significant changes in Phd3 mRNA between P0 and any age examined (multiple comparisons test all P values >0.05). In the ACX, there was an increase in Phd3 mRNA levels between P0 and P21 in ACX of low-LG samples (multiple comparisons test $P=0.0260$).

Figure 8C shows developmental expression profiles for the kinase mTor, and secreted signaling protein isoforms Wnt7a and Wnt7b. The relative levels of mTor mRNA in the CN and pons did not change between P0 and any age tested (one-way ANOVA $P=0.2815$, $P=0.7722$ for CN and pons, respectively). In the IC and ACX, there were increases in both LG groups between P0 and P21 (one-way ANOVA $P=0.1119$, $P=0.0056$ for IC and ACX, respectively; multiple comparisons test $P=0.0334$, $P=0.0210$ for low-LG and high-LG groups in IC, respectively; $P=0.0056$, $P=0.0005$ for low-LG and high-LG groups in ACX, respectively). Lastly, in the VCX, there were increases in high-LG pups between P0 and P15 (one-way ANOVA $P=0.0015$; multiple comparisons test $P=0.0057$), and in both LG groups between P0 and P21 (multiple comparisons test $P=0.0012$, $P=0.0007$ for low-LG and high-LG samples, respectively). The developmental profile of Wnt7a mRNA in the CN, pons, and VCX, did not show any changes between P0 and any age examined (one-way ANOVA $P=0.0682$, $P=0.5819$, $P=0.1640$ for CN, pons and VCX, respectively). In the IC, there was an increase in Wnt7a mRNA in low-LG pups between P0 and P21 (one-way ANOVA $P=0.0125$; multiple comparisons test $P=0.0023$), and in the ACX, there were increases in Wnt7a mRNA in both LG groups between P0 and P21 (one-way ANOVA $P=0.0153$; multiple comparisons test $P=0.0102$, $P=0.0059$ for low-LG and high-LG samples, respectively). Lastly, there were no changes in Wnt7b mRNA levels between P0 and any age tested in any of the brain regions tested (one-way ANOVA $P=0.1389$, $P=0.2215$, $P=0.2004$, $P=0.4577$, $P=0.6010$ for CN, pons, IC, ACX and VCX, respectively).

In sum, the data in **Figure 8** shows evidence that genes involved in myelin development and two signaling pathways, the hypoxia-sensitive pathway and the mTor/Wnt7 pathway, showed

heterogeneous changes, increasing between P0 and P15, between P0 and P21, or remaining constant throughout the ages examined. It is notable that mRNA levels for Phd2 showed a decrease between P0 and P7, and between P0 and P15 in most auditory brain regions examined, but not in the VCX.

Analysis of genes involved in cell signaling, water diffusion, and ion diffusion

Figure 9 shows the developmental profiles of mRNAs coding for diverse membrane proteins involved in cell signaling, water, and ion diffusion. **Figure 8A** shows developmental profiles for the glutamate transporter VGluT3, the water channel AQP4, the voltage-dependent potassium channel Kv1.3 and the voltage and calcium sensitive chloride channel TMEM16a. The developmental profile of expression for VGluT3 mRNA did not show changes between P0 and any age tested in the CN, IC, ACX, and VCX (one-way ANOVA $P=0.4894$, $P=0.4882$, $P=0.4543$, $P=0.7512$ for CN, IC, ACX and VCX, respectively). In the pons, VGluT3 mRNA decreased between P0 and P15 in both LG groups (one-way ANOVA $P=0.1447$; multiple comparisons $P=0.0126$, $P=0.0189$ for low-LG and high-LG samples, respectively). The developmental profile of Aqp4 mRNA expression in the CN showed increases between P0 and P7 in high-LG pups (one-way ANOVA $P=0.0001$; multiple comparisons test $P=0.0402$), between P0 and P15 in both LG groups (multiple comparisons test $P=0.0012$, $P=0.0024$ for low-LG and high-LG samples, respectively), and between P0 and P21 in both LG groups (multiple comparisons test $P=0.0001$, $P=0.0001$). In the pons, IC, ACX and VCX, there were consistent increases in Aqp4 mRNA between P0 and P15 (one-way ANOVA $P=0.0022$, $P=0.0010$, $P=0.0001$, $P=0.0001$; multiple comparisons test $P=0.0429$, $P=0.0248$ for low-LG and high-LG samples in pons, respectively; multiple comparisons test $P=0.0366$, $P=0.0079$ for low-LG and high-LG samples in IC, respectively; multiple comparisons test $P=0.0030$, $P=0.0037$ for low-LG and high-LG samples in ACX, respectively; multiple comparisons test $P=0.0143$, $P=0.0090$ for low-LG and high-LG samples in VCX, respectively), and between P0 and P21 (multiple

comparisons test $P=0.0006$, $P=0.0008$ for low-LG and high-LG samples in pons, respectively; multiple comparisons test $P=0.0003$, $P=0.0003$ for low-LG and high-LG samples in IC, respectively; multiple comparisons test $P=0.0001$, $P=0.0001$ for low-LG and high-LG samples in ACX, respectively; multiple comparisons test $P=0.0001$, $P=0.0001$ for low-LG and high-LG samples in VCX, respectively). The developmental expression profile for Kv1.3 mRNA in the CN, pons, IC, and VCX, did not show changes between P0 and any age tested (one-way ANOVA $P=0.2693$, $P=0.6529$, $P=0.2559$, $P=0.3509$ for CN, pons, IC and VCX, respectively). There was an increase in the ACX between P0 and P21 in high-LG samples (one-way ANOVA $P=0.1153$; multiple comparisons test $P=0.0093$). The developmental expression profile of TMEM16a mRNA in the CN, pons, IC, ACX, and VCX, did not show any changes between P0 and any age tested (one-way ANOVA $P=0.0111$, $P=0.5035$, $P=0.6650$, $P=0.4616$, $P=0.3545$ in CN, pons, IC, ACX and VCX, respectively).

Figure 9B shows the developmental expression profiles of Pannexin1 and Pannexin2 mRNAs. In the CN, pons, IC, ACX, and VCX, Pannexin1 mRNA levels did not show any changes between P0 and any age tested (one-way ANOVA $P=0.0237$, $P=0.1686$, $P=0.6542$, $P=0.8059$, $P=0.4887$ for CN, pons, IC, ACX, and VCX, respectively). The developmental profile of Pannexin2 mRNA did not show changes in auditory brainstem structures between P0 and any age tested (one-way ANOVA $P=0.8168$, $P=0.5977$, $P=0.3431$ for CN, pons, and IC, respectively). In contrast, in the ACX there were increases between P0 and P15 in high-LG pups (One way ANOVA $P=0.0124$; multiple comparisons test $P=0.0272$), and in VCX between P0 and P15 in both LG groups (one-way ANOVA $P=0.0189$; multiple comparisons test $P=0.0226$, $P=0.0469$ for low-LG and high-LG samples, respectively). Lastly, in the ACX and VCX, there were increases between P0 and P21 in both LG groups (multiple comparisons test $P=0.0363$, $P=0.0076$ in low-LG and high-LG groups in ACX, respectively; $P=0.0072$, $P=0.0146$ in low-LG and high-LG groups in VCX, respectively).

741

742 **Figure 9C** shows developmental expression profiles for the mRNAs of gap junction connexin

743 subunits Cx36, Cx37, Cx40 and Cx43. In the CN, pons, IC, and VCX, the developmental profile

744 of Cx36 expression did not show changes between P0 and any age tested (one-way ANOVA

745 $P=0.4181$, $P=0.6722$, $P=0.8983$, $P=0.9273$ for CN, pons, IC and VCX, respectively). In contrast,

746 there were increases in the ACX between P0 and P7 in high-LG pups (one-way ANOVA

747 $P=0.0202$; multiple comparisons test $P=0.0144$), between P0 and P15 in high-LG pups (multiple

748 comparisons test $P=0.0012$), and between P0 and P21 in both LG groups (multiple comparisons

749 test $P=0.0089$, $P=0.0032$ for low-LG and high-LG samples, respectively). The developmental

750 profile of expression of Cx37 mRNA did not show any changes in the CN, pons, IC, ACX, and

751 VCX, between P0 and any age tested (one-way ANOVA $P=0.0245$, $P=0.3028$, $P=0.5237$,

752 $P=0.5951$, $P=0.8205$ for CN, pons, IC, ACX and VCX, respectively). Similarly, in the CN, pons,

753 IC, ACX, and VCX, the expression levels of Cx40 mRNA did not show any changes between P0

754 and any age tested (one-way ANOVA $P=0.1392$, $P=0.4419$, $P=0.4332$, $P=0.1673$, $P=0.0261$ for

755 CN, pons, IC, ACX and VCX, respectively). In the CN, pons, and VCX, Cx43 mRNA levels

756 showed increases between P0 and P21 in both LG groups (one-way ANOVA $P=0.0098$,

757 $P=0.0001$, $P=0.0045$; multiple comparisons test $P=0.0145$, $P=0.0070$ for low-LG and high-LG

758 samples in CN, respectively; $P=0.0001$, $P=0.0001$ for low-LG and high-LG samples in pons,

759 respectively; $P=0.0099$, $P=0.0006$ for low-LG and high-LG samples in VCX, respectively). In

760 the IC, there was an increase between P0 and P21 in high-LG samples (one-way ANOVA

761 $P=0.0393$; multiple comparisons test $P=0.0058$). Lastly, in the ACX, there were increases in both

762 LG groups between P0 and P15 (one-way ANOVA $P=0.0001$; multiple comparisons test

763 $P=0.0012$, $P=0.0001$ for low-LG and high-LG samples, respectively), and between P0 and P21

764 (multiple comparisons test $P=0.0001$, $P=0.0001$ for low-LG and high-LG samples, respectively).

765

766 In sum, the data in **Figure 9** shows evidence that the mRNA levels for several transmembrane
767 proteins involved in cell signaling, water and ion diffusion did not change significantly between
768 P0 and other ages examined. The exception was Aqp4 mRNA, which showed consistent
769 increases between P0 and P15, and between P0 and P21 in all brain regions examined.

DISCUSSION

In this study we hypothesized that differences in maternal licking and grooming (LG) during the first week of life are associated with differences in the timing of hearing onset. However, the results of this study do not support the hypothesis, and indicate that different levels of maternal LG are not sufficient to modulate hearing onset in the progeny (**Figures 2 and 3**). Nevertheless, this study provides three new findings concerning auditory development: First, it shows that early onset of functional responses correlates with a variable delay to eye opening (EO; **Figure 4**); second, it adds new information on the relationship between the formation of the middle ear cavity and the threshold of functional responses during hearing onset (**Figures 5 and 6**); and third, it shows for the first time that mRNAs of the hypoxia sensitive pathway and the BDNF/TrkB signaling pathway are regulated before and after the onset of hearing, respectively (**Figures 7-9**). Following is a discussion of the merits and limitations of these findings, including considerations for future studies.

Variable delay between early hearing onset and EO

A major caveat of the approach used in the present study is that we were not able to predict the developmental profile of individual litters based on maternal LG. However, we were surprised to find that litters reared by low-LG and high-LG dams showed a similar range of early and late auditory brainstem response (ABR) onset. This turned out to be an advantage, because by tracking pups during development we were able to measure the delay between ABR onset and EO in a relatively large number of litters. The onset of hearing for airborne sounds precedes EO, and this sequence of events occurs prenatally or postnatally in different vertebrate species. The finding that litters with an early ABR onset have a more variable delay to EO (**Figure 4**) is relevant in the context of recent studies that manipulated the timing of EO and measured its effects on the development of membrane and synaptic properties of primary auditory cortex neurons in gerbils, and of synaptic properties of primary visual cortex neurons in Long-Evans

rats (Mowery et al., 2016; Tatti et al., 2017). We propose that a better understanding of the relationship between hearing onset and the delay to EO will be useful to study cross modal experience-dependent plasticity between visual and auditory systems in rodents. Studies are needed to characterize the signaling pathways that influence the development of feed-forward and feedback mechanisms between ACX and VCX in animals with early and late hearing onset (Budinger et al., 2006; Mowery et al., 2016; Pan et al., 2018).

Relationship between development of the auditory periphery and development of sensorineural responses from the inner ear

Combined functional and structural analyses from this study showed that cavity formation in the middle ear correlated with the type of sensorineural responses tracked in animals of different ages. We found that within a range of air volume from 15 mm³ to 40 mm³, ABRs had very elevated click intensity thresholds and relatively simple waveforms (**Figures 5 and 6**). For example, short latency potentials (SLPs) predominated over wave I responses at P12, and SLPs gradually waned as wave I responses increased in amplitude at P13 (**Figure 6**). Our results have confirmed and expanded on the previous findings of Blatchley, Cooper and Coleman, who described similar short latency responses to tone pips in ether-anesthetized P12 Sprague-Dawley rat pups (referred as summing potentials in their Figure 2: Blatchley, Cooper and Coleman, 1987). Additionally, it is puzzling to us that SLPs were observed without wave I responses, and that wave I responses were observed without subsequent ABR wave components II-V. Given the accumulating evidence that hair cells and neurons along the entire auditory system are functionally connected and active prior to hearing onset in different vertebrate species (Lippe, 1994; Gummer and Mark, 1994; Jones et al., 2007; Sonntag et al., 2009; Tritsch et al., 2010; Johnson et al., 2012; Babola et al., 2018; Corns et al., 2018), it is reasonable to propose that the functional changes observed in this study could reflect the contribution of conductive development to increased sensitivity (Saunders, Doan and Cohen, 1993), and the suppressive

effects of isoflurane anesthesia on auditory function (Ruebhausen, Brozoski and Bauer, 2012; Bielefeld, 2014; Sheppard, Zhao, and Salvi, 2018). Future studies are needed to address how functional parameters of early sensory responses are affected by the state of the animal. This will require implementation of innovative methods to track structural and functional changes in non-anesthetized pups as they grow during postnatal development.

Postnatal changes in gene expression of signaling pathways

The first postnatal weeks represent a sequence of sensitive periods when expression of genes involved in cellular proliferation, migration, differentiation, synaptogenesis, myelination, apoptosis, and neuroplasticity are regulated temporally and regionally in the CNS. The onset of ABRs and EO represent developmental stages in which auditory and visual experience can affect the above cellular processes in sensory pathways. In this study we found evidence that the hypoxia-sensitive pathway and the BDNF/TrkB pathway are regulated before and after the onset of hearing, respectively.

The hypoxia-sensitive pathway regulates gene expression by a negative feedback mechanism that is sensitive to a reduction in O₂ partial pressure (i.e., hypoxia). O₂ sensing is mediated by Phd paralogues that interact with hypoxia-inducible factors Hif1a and Hif2a to target them for degradation in normoxic conditions. During hypoxic conditions Phd/Hif interactions decrease, reducing Hif degradation and increasing Hif stability that enables the transcriptional activation of the erythropoietin gene by Hif2a, and the transcriptional regulation of genes encoding glycolytic enzymes by Hif1a (reviewed in Lappin and Lee, 2019). In this study we found that Phd2 mRNA was down regulated in auditory brain regions before and after the onset of hearing and EO, while mRNAs for Hif1a, Hif2a, Phd1 and Phd3 did not change, or increased at ages posterior to hearing onset (**Figure 8B**). This finding is intriguing to us and raises several questions for future studies: First, do cells that down regulate Phd2 increase Hif activity? What causes down

regulation of Phd2 mRNA? What are the consequences of activating the Hif pathway during development of auditory brain regions? We propose that a first step to answer these questions will require localization of Hif and Phd mRNA and protein to specific cell types throughout the auditory system.

The BDNF signaling pathway is involved in neuronal survival, cell growth, and differentiation via activation of its tyrosine kinase receptor TrkB, which in turn can modulate several signaling pathways including Akt/PI3K, Jak/STAT, NF- κ B, UPAR/UPA, Wnt/ β -catenin, and VEGF (Tajbakhsh et al., 2017). Studies in primary auditory cortex (ACX) and primary visual cortex (VCX) of rats and a mouse model of fragile X have shown that BDNF/TrkB signaling is regulated by sensory experience (Bozzi et al., 1995; Berardi, Pizzorusso and Maffei, 2000; Wang et al., 2017; Kulinich et al., 2019). In this study, we found a significant increase in mRNAs for TrkB, NF κ B, Akt2, and Wnt7a in the ACX and VCX after hearing onset and EO (**Figures 7 and 8C**; although Wnt7a did not change in VCX). Furthermore, changes in mRNAs for TrkB and NF κ B in the ACX were significantly different between pups reared by low-LG and high-LG dams at P21. These results expand previous findings that maternal care strongly modulates brain BDNF levels in rodents (Branchi et al., 2013; Liu et al., 2000), and implicate maternal LG in experience-dependent development of functional responses in primary auditory cortex (de Villers-Sidani and Merzenich, 2011).

Lastly, in this study we found evidence of mRNA upregulation of alternative signaling pathways involving c-Jun, Akt1, and Sort1 in subcortical auditory brain regions during a stage that coincides with the maturation of auditory thresholds and the end of the critical period for frequency tuning (Adise et al., 2014; de Villers-Sidani and Merzenich, 2011). Altogether, these results indicate a robust range of auditory periphery development and eye opening in Wistar rat

873 pups that experience variation in maternal backgrounds. Consistent with this interpretation, there
874 is a robust change in brain gene expression of Ph2, a crucial component of the hypoxia sensitive
875 pathway, before hearing onset. In addition, the results of this study implicate maternal LG in the
876 expression of molecular factors involved in experience-dependent plasticity, neural signaling and
877 transcriptional control in subcortical and cortical sensory brain regions of the progeny. Despite
878 previous findings that maternal LG is increased in adoptive Wistar rat dams (Maccari et al.,
879 1995), and that massage treatment during the sensitive period before eye opening (EO)
880 accelerates development of visually evoked potentials in Long-Evans rats (Guzzeta et al., 2009),
881 it is unlikely that increased physical stimulation through LG can explain the effects of maternal
882 separation on ABR and middle ear development reported previously in Wistar rat pups (Adise et
883 al., 2014).

884 REFERENCES

885 Adise S, Saliu A, Maldonado N, Khatri V, Cardoso L, Rodríguez-Contreras A (2014) Effect of
886 maternal care on hearing onset induced by developmental changes in the auditory periphery. J
887 Neurosci 34(13): 4528-4533.

888
889 Babola TA, Li S, Gribizis A, Lee BJ, Issa JB, Wang HC, Crair MC, Bergles DE (2018)
890 Homeostatic control of spontaneous activity in the developing auditory system. Neuron 99(3):
891 511-524.

892
893 Barha CK, Pawluski JL, Galea LA (2007) Maternal care affects male and female offspring
894 working memory and stress reactivity. Physiol Behav 92(5): 939-950.

895
896 Berardi N, Pizzorusso T, Maffei L (2000) Critical periods during sensory development. Curr
897 Opin Neurobiol 10(1): 138-145.

898
899 Bielefeld EC (2014) Influence of dose and duration of isoflurane anesthesia on the auditory
900 brainstem response in the rat. Int J Audiol 53: 250-258.

901
902 Blatchely BJ, Cooper WA, Coleman JR (1987) Development of auditory brainstem response to
903 tone pip stimuli in the rat. Brain Res 429: 75-84.

904
905 Bogaerts S, Clements JD, Sullivan JM, Oleskevich S (2009) Automated threshold detection for
906 auditory brainstem responses: comparison with visual estimation in a stem cell transplantation
907 study. BMC Neurosci 10: 104.

908

909 Bozzi Y, Pizzorusso T, Cremisi F, Rossi FM, Barsacchi G, Maffei L (1995) Monocular
 910 deprivation decreases the expression of messenger RNA for brain-derived neurotrophic factor in
 911 the rat visual cortex. *Neuroscience* 69(4): 133-1144.
 912
 913 Branchi I, Curley JP, D'Andrea I, Cirulli F, Champagne FA, Alleva E (2013) Early interactions
 914 with mother and peers independently build adult social skills and shape BDNF and oxytocin
 915 receptor brain levels. *Psychoneuroendocrinol* 38: 522-532.
 916
 917 Budinger E, Heil P, Hess A, Scheich H (2006) Multisensory processing via early cortical stages:
 918 connections of the primary auditory cortical field with other sensory systems. *Neuroscience* 143:
 919 1065-1083.
 920
 921 Cameron N, Del Corpo A, Diorio J, McAllister K, Sharma S, Meaney MJ (2008) Maternal
 922 programming of sexual behavior and hypothalamic-pituitary-gonadal function in the female rat.
 923 *PLoS One* 3(5): e2210.
 924
 925 Careaga M, Murai T, Bauman MD (2017) Maternal immune activation and autism spectrum
 926 disorders: From rodents to nonhuman and human primates. *Biol Psychiatry* 81(5): 391-401.
 927
 928 Champagne FA, Francis DD, Mar A, Meaney MJ (2003) Variations in maternal care in the rat as
 929 a mediating influence for the effects of environment on development. *Physiol Behav* 79(3): 359-
 930 371.
 931
 932 Corns LF, Johnson SL, Roberts T, Ranatunga KM, Hendry A, Ceriani F, Safieddine S, Steel KP,
 933 Forge A, Petit C, Furness DN, Kros CJ, Marcotti W (2018) Mechanotransduction is required for

934 establishing and maintaining mature inner hair cells and regulating efferent innervation. Nat
 935 Comm 9(1): 4015.
 936
 937 Curley JP, Champagne FA (2016) Influence of maternal care on the developing brain:
 938 mechanisms, temporal dynamics and sensitive periods. Front Neuroendocrinol 40: 52-66.
 939
 940 de Villers-Sidani E, Merzenich MM (2011) Lifelong plasticity in the rat auditory cortex: Basic
 941 mechanisms and role of sensory experience. In Green AM, Chapman E, Kalaska JF, Lepore F,
 942 Editors: Prog Brain Res 191: 119-131.
 943
 944 Francis D, Diorio J, Liu D, Meaney MJ (1999) Nongenomic transmission across generations of
 945 maternal behavior and stress responses in the rat. Science 286: 1155-1158.
 946
 947 González-Mariscal G, Melo AI (2017) Bidirectional effects of mother-young contact on the
 948 maternal and neonatal brains. Adv Exp Med Biol 1015: 97-116.
 949
 950 Gummer AW, Mark RF (1994) Patterned neural activity in brain stem auditory areas of a
 951 prehearing mammal, the tammar wallaby *Macropus eugenii*. Neuroreport 5: 685-688.
 952
 953 Guzzetta A, Baldini S, Bancale A, Baroncelli L, Ciucci F, Ghirri P, Putignano E, Sale A, Vieg
 954 A, Berardi N, Boldrini A, Cioni G, Maffei L (2009) Massage accelerates brain development and
 955 the maturation of visual function. J Neurosci 29: 6042-6051.
 956
 957 Hancock SD, Menard JL, Olmstead MC (2005) Variations in maternal care influence
 958 vulnerability to stress-induced binge eating in female rats. Physiol Behav 85(4): 430-439.
 959

960 Johnson SL, Kennedy HJ, Holley MC, Fettiplace R, Marcotti W (2012) The resting transducer
 961 current drives spontaneous activity in prehearing mammalian cochlear inner hair cells. *J*
 962 *Neurosci* 32(31): 10479-10483.
 963
 964 Jones TA, Leake PA, Snyder RL, Stakhovskaya O, Bonham B (2007) Spontaneous discharge
 965 patterns in cochlear spiral ganglion cells before the onset of hearing in cats. *J Neurophysiol* 98:
 966 1898-1908.
 967
 968 Kulinich AO, Reinhard SM, Rais M, Lovelace JW, Scottt V, Binder DK, Razak KA, Ethell IM
 969 (2019) Beneficial effects of sound exposure on auditory cortex development in a mouse model of
 970 fragile X syndrome. *Neurobiol Dis* 134: 104622.
 971
 972 Lappin TR, Lee FS (2019) Update on mutations in the HIF: EPO pathway and their role in
 973 erythrocytosis. *Blood Rev* 37: 100590.
 974
 975 Lippe WR (1994) Rhythmic spontaneous activity in the developing avian auditory system. *J*
 976 *Neurosci* 14: 1486-1495.
 977
 978 Liu D, Diorio J, Tanenbaum B, Caldji C, Francis D, Freedman A, Sharma S, Pearson D, Plotsky
 979 PM, Meaney MJ (1997) Maternal care, hippocampal glucocorticoid receptors, and hypothalamic-
 980 pituitary-adrenal responses to stress. *Science* 277: 1659-1662.
 981
 982 Liu D, Diorio J, Day JC, Francis DD, Meaney MJ (2000) Maternal care, hippocampal
 983 synaptogenesis and cognitive development in rats. *Nature Neurosci* 3: 799-806.
 984

985 Maccari S, Piazza PV, Kabbaj M, Barbazanges A, Simon H, Le Moal M (1995) Adoption
986 reverses the long-term impairment in glucocorticoid feedback induced by prenatal stress. *J*
987 *Neurosci* 15: 110-116.

988

989 Menard JL, Hakvoort RM (2007) Variations of maternal care alter offspring levels of
990 behavioural defensiveness in adulthood: evidence for a threshold model. *Behav Brain Res*
991 176(2): 302-313.

992

993 Mowery TM, Kotak VC, Sanes DH (2016) The onset of visual experience gates auditory cortex
994 critical periods. *Nat Commun* 7: 10416.

995

996 Mulder JJ, Kuijpers W, Peters TA, Tonnaer EL, Ramaekers FC (1998) Development of the
997 tubotympanum in the rat. *Laryngoscope* 108: 1846-1852.

998

999 Pan P, Zhou Y, Fang F, Zhang G, Ji Y (2018) Visual deprivation modifies oscillatory activity in
1000 visual and auditory centers. *Anim Cells Sys (Seoul)* 22: 149-156.

1001

1002 Parent CI, Meaney MJ (2008) The influence of natural variations in maternal care on play
1003 fighting in the rat. *Dev Psychobiol* 50(8): 767-776.

1004

1005 Rothman JS, Silver RA (2018) NeuroMatic: An integrated open-source software toolkit for
1006 acquisition, analysis and simulation of electrophysiological data. *Front Neuroinform* 12: 14.

1007

1008 Ruebhausen MR, Brozoski TJ, Bauer CA (2012) A comparison of the effects of isoflurane and
1009 ketamine anesthesia on auditory brainstem response (ABR) thresholds in rats. *Hear Res* 287: 25-
1010 29.

1011

1012 Sakhai SA, Kriegsfeld LJ, Francis DD (2011) Maternal programming of sexual attractivity in

1013 female Long Evans rats. *Psychoneuroendocrinology* 36(8): 1217-1225.

1014

1015 Salmaso N, Jablonska B, Scafidi J, Vaccarino FM, Gallo V (2014) Neurobiology of premature

1016 brain injury. *Nat Neurosci* 17(3):341-346.

1017

1018 Saunders JC, Doan DE, Cohen YE (1993) The contribution of middle-ear sound conduction to

1019 auditory development. *Comp Biochem Physiol Comp Physiol* 106: 7-13.

1020

1021 Sheppard AM, Zhao D-L, Salvi R (2018) Isoflurane anesthesia suppresses distortion product

1022 otoacoustic emissions in rats. *J Otol* 13: 59-64.

1023

1024 Sonntag M, Englitz B, Kopp-Scheinflug C, Rubsamen R (2009) Early postnatal development of

1025 spontaneous and acoustically evoked discharge activity of principal cells of the medial nucleus

1026 of the trapezoid body: an in vivo study in mice. *J Neurosci* 29(30): 9510-9520.

1027

1028 Tajbakhsh A, Mokhtari-Zaer A, Rezaee M, Afzaljavan F, Rivandi M, Hassanian SM, Ferns GA,

1029 Pashar A, Avan A (2017) Therapeutic potentials of BDNF-TrkB in breast cancer; current status

1030 and perspectives. *J Cell Biochem* 118: 2502-2515.

1031

1032 Tatti R, Swanson OK, Lee MSE, Maffei A (2017) Layer-specific developmental changes in

1033 excitation and inhibition in rat primary visual cortex. *eNeuro* 4(6).

1034

1035 Tritsch NX, Rodríguez-Contreras A, Crins TT, Wang HC, Borst JGG, Bergles DE (2010)

1036 Calcium action potentials in hair cells pattern auditory neuron activity before hearing onset. *Nat*

1037 *Neurosci* 13(9): 1050-1052.

1038

1039 Walker CD, Xu Z, Rochford J, Johnston CC (2008) Naturally occurring variations in maternal

1040 care modulate the effects of repeated neonatal pain on behavioral sensitivity to thermal pain in

1041 the adult offspring. *Pain* 140(1): 167-176.

1042

1043 Wang Y, Ou X, Liu Y, Lu H (2017) Auditory deprivation modifies the expression of brain-

1044 derived neurotrophic factor and tropomyosin receptor kinase B in the rat auditory cortex. *J Otol*

1045 12: 34-40.

1046

1047 Weaver IC, Cervoni N, Champagne FA, D'Alessio AC, Sharma S, Seckl JR, Dymov S, Szyf M,

1048 Meaney MJ (2004) Epigenetic programming by maternal behavior. *Nat Neurosci* 7: 847-854.

1050 **Figure 1. Experimental approach.** **A**, The percent of pups with an auditory brainstem response
 1051 (ABR) or eye opening (EO) in a litter increases as a function of age. Fitting such data to equation
 1052 1 determines an A_{50} value, the age at which 50% of pups in a litter show an ABR or EO. In this
 1053 study we test the hypothesis that variation in maternal licking and grooming (LG) is associated
 1054 with pup's early (dashed line a) and late (continuous line b) sensory development profiles. **B**,
 1055 Four maternal selection experiments were performed during spring and summer seasons (2
 1056 replicates per season, with cohorts of 40 dams per experiment). After dams gave birth (P0)
 1057 maternal behavior was scored daily from P1 to P6 (n=135 dams). ABRs were tracked daily in all
 1058 pups from seventeen selected litters between P10 and P15, and at P21. EO was tracked daily
 1059 between P10 and P21 (n=199 pups). **C**, After behavioral scoring and selection between P1 and
 1060 P6, correlative ABR and micro-CT X-ray tomography measurements were obtained from two
 1061 low-LG litters (n=14 pups) and from two high-LG litters (n=15 pups) between P10 and P15
 1062 (indicated by arrowheads). **D**, Brain samples were obtained at different ages for gene expression
 1063 analysis, prior and after behavioral scoring from three low-LG litters and four high-LG litters at
 1064 P7, P15, and at P21 (indicated by arrowheads). Three litters were used to collect pups at P0,
 1065 which was defined as a baseline for expressing fold changes in gene expression at other ages
 1066 (n=3 pups per age per LG condition).

Figure 2. Variation in licking and grooming (LG) across different dam cohorts. **A**, Box plots of six-day average LG scores from cohorts analyzed in the spring and summer of two consecutive years. Each circle represents one dam. Asterisks indicate P values obtained by Holm's Sidak's multiple comparisons test, **=0.0021, ***=0.0001 and 0.0005, ****<0.0001. **B**, Daily LG scores for seven low-LG dams selected from spring and summer cohorts (continuous lines and dashed lines, respectively). **C**, Daily LG scores for ten high-LG dams selected from spring and summer cohorts (continuous lines and dashed lines, respectively). **D**, Six-day average LG scores for low LG and high-LG dams selected from spring and summer cohorts. Each circle represents one dam. Asterisks indicate P values obtained by Tukey's multiple comparisons test, *=0.0249, **=0.0035 and 0.0088, ****<0.0001. n.s.=not significant.

Figure 3. Timing of auditory brainstem response (ABR) onset and eye opening (EO) in the offspring of selected dams. **A**, Plots of percent pups with ABR wave I at different ages from seven low-licking and grooming (low-LG) litters were fit to equation 1. **B**, Plots of percent pups with ABR wave I at different ages from ten high-licking and grooming (high-LG) litters were fit to equation 1. **C**, Plots of percent pups with EO at different ages from seven low-LG litters were fit to equation 1. **D**, Plots of percent pups with EO at different ages from ten high-LG litters were fit to equation 1. **E**, Violin plots of A_{50} values obtained from fits of equation 1 to developmental data of percent pups with ABR or EO. **F**, Violin plots of rate coefficient k values obtained from fits of equation 1 to developmental data of percent pups with ABR or EO. Asterisks indicate significant differences between medians: * indicates P value = 0.0172; ** indicate P values = 0.0055 and 0.0027; *** indicates P value = 0.0005; Dunn's multiple comparisons test; n.s.=not significant. Continuous lines represent fits to spring litters; dashed lines represent fits to summer litters.

Figure 4. Delay between auditory brainstem response (ABR) onset and eye opening (EO).
A, Scatter plot of A_{50} values show the relationship between EO and ABR onset in low-licking and grooming (low-LG) and high-licking and grooming (high-LG) litters. **B,** Scatter plot of rate coefficient k values show the relationship between EO and ABR development in selected low-LG and high-LG litters. Magenta symbols represent low-LG data; blue symbols represent high-LG data. Black line in A and B represents the identity line.

Figure 5. Relationship between development of the middle cavity and wave 1 auditory brainstem (ABR) thresholds. **A**, Top, developmental series of micro-CT X ray scans of pups from a low-licking and grooming (low-LG) litter. White indicates bone, grey is soft tissue and black is air. Bottom, 3D rendering of segmented bone (gray) and air (purple) contrast obtained from tomographic data. **B**, Air volume measured at different ages in pups from two low-LG (magenta) and two high-licking and grooming (high-LG) litters (blue). Note that every symbol represents one pup and that similar symbols represent pups from the same litter. Continuous and dotted color lines are fits of equation 1 to the data. **C**, Relationship between ABR wave I thresholds and air volume in the middle ear cavity. Magenta circles and triangles represent pups from low-LG litters (n = 25 pups); blue circles and triangles represent pups from high LG litters (n = 26 pups). NR = non-responsive pups, defined by the absence of ABR wave I. Black line represents the fit to a linear function between wave I thresholds and air volume with slope 2.5 dB/mm³. Symbols with white dots indicate data points included in the fit.

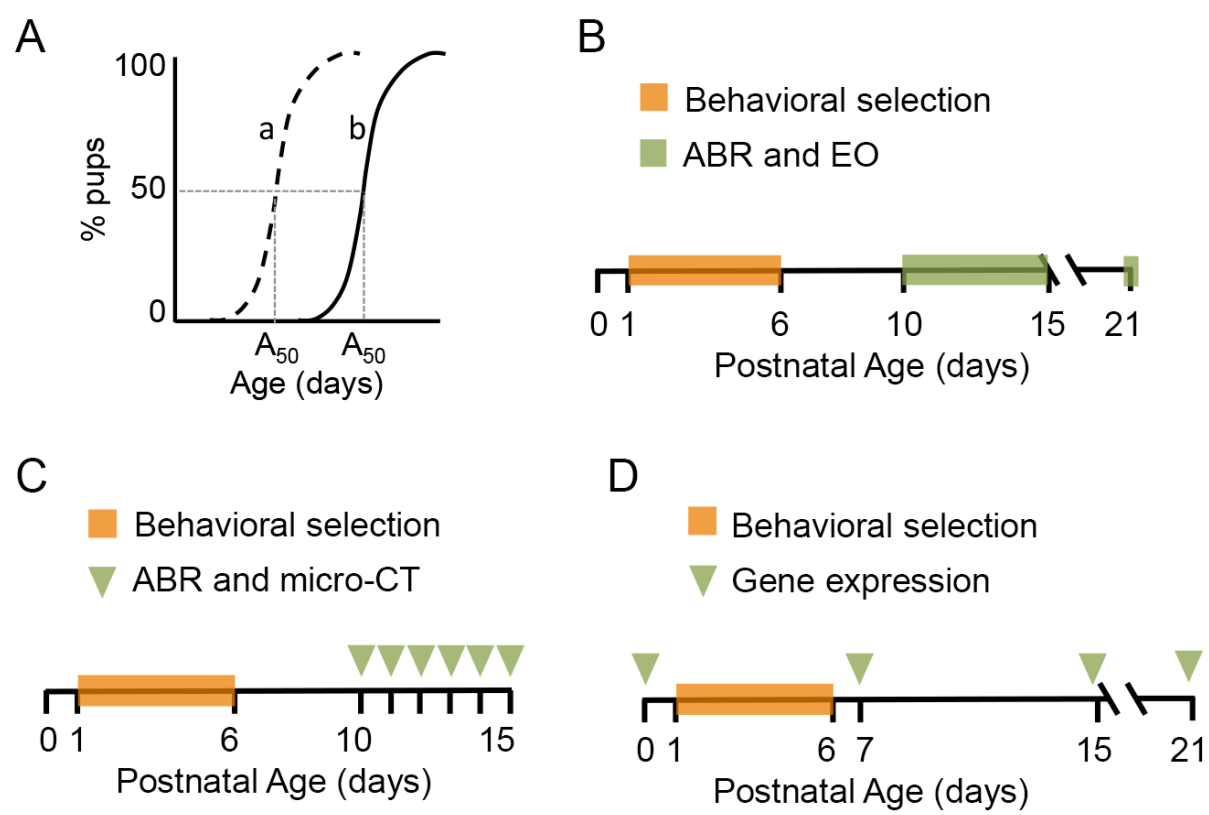
Figure 6. Identification of short latency potentials (SLPs) in combined auditory brainstem response (ABR) and micro-CT X ray (micro-CT) experiments. **A, C, E,** Representative 3D rendering of three P12 pups with different volumes of air in the middle ear and external canal. **B, D, F,** Corresponding ABR waveforms show the presence of a SLP in pups with air volumes of 24 mm³ and 36 mm³, but not in the pup without middle ear and external ear cavities. ABR traces in B, D and F correspond to click intensities shown in panel F. **G,** SLP thresholds as a function of air volume. Black line represents the fit to a linear function between SLP thresholds and air volume with slope 0.3 dB/mm³. Symbols with white dots indicate data points included in the fit. **H,** Comparison of SLP thresholds and wave 1 thresholds for pups measured at P12 and P13. Filled symbols represent pups used in combined ABR and micro-CT experiments. Open symbols are littermates used solely in ABR experiments at P12. Asterisks indicate pups tracked from P12 to P13. Black dashed line in H is the identity line. Arrows in G and H indicate a pup that showed ABR wave I but not a SLP.

Figure 7. Developmental gene expression profiles for genes involved in neural development and plasticity. **A,** Relative level of mRNA expression of neurotrophin genes BDNF, NGF and the BDNF receptor TrkB. **B,** Relative level of mRNA expression for transcription factors c-Fos, c-Jun, NFκB and Otx2. **C,** Relative level of mRNA expression for signaling effectors Akt1, Akt2, and Sort 1. Data is plotted as fold change with respect to birth (P0). Magenta symbols represent data from low-licking and grooming (low-LG) samples. Blue symbols represent data from high-licking and grooming (high-LG) samples. Data represents mean \pm sem (n=3 pups per age per LG group). Asterisks represent statistically significant differences determined by multiple comparisons test. Boxed data represents statistically significant differences between low-LG and high-LG samples. Alpha=0.05.

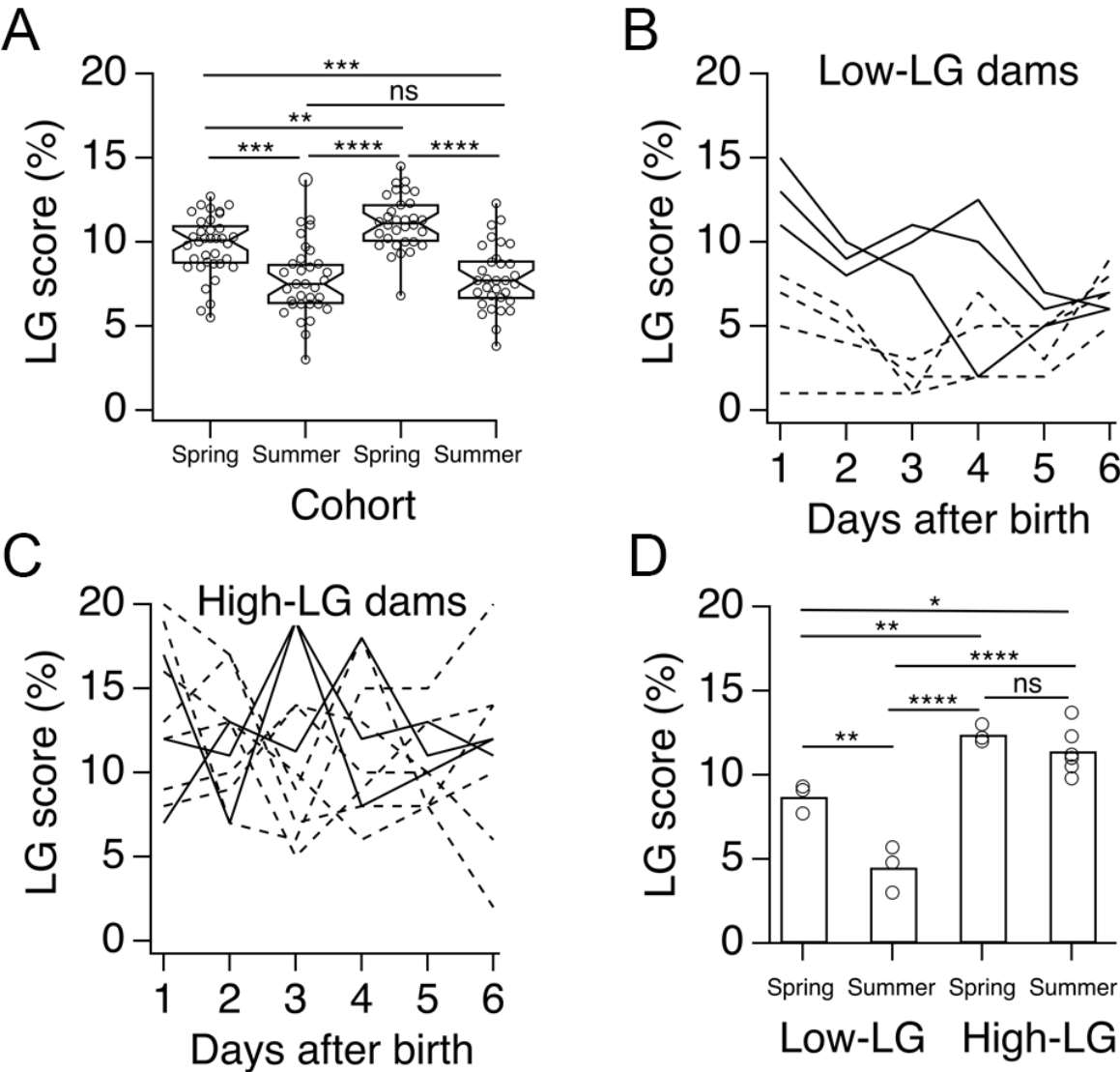
Figure 8. Developmental gene expression profiles for genes involved in myelin development, the hypoxia-sensitive pathway and the mTor/Wnt7 pathway. **A**, Relative level of mRNA expression of Olig2 and Mbp. **B**, Relative level of mRNA expression of Hif1a, Hif2a, and Phd isoforms 1, 2 and 3. **C**, Relative level of mRNA expression of mTor, Wnt7a and Wnt7b. Magenta symbols represent data from low-licking and grooming (low-LG) samples. Blue symbols represent data from high-licking and grooming (high-LG) samples. Data represents mean \pm sem (n=3 pups per age per LG group). Asterisks represent statistically significant differences determined by multiple comparisons test. Alpha=0.05.

Figure 9. Developmental gene expression profiles for genes involved in neural signaling. A, Relative level of mRNA expression of Vglut3, Aqp4, Kv1.3, and TMEM16a. **B,** Relative level of mRNA expression of Panexin1 and Pannexin2. **C,** Relative level of mRNA expression of Cx36, Cx37, Cx40 and Cx43. Magenta symbols represent data from low-licking and grooming (low-LG) samples. Blue symbols represent data from high-licking and grooming (high-LG) samples. Data represents mean \pm sem (n=3 pups per age per LG group). Asterisks represent statistically significant differences determined by multiple comparisons test. Alpha=0.05.

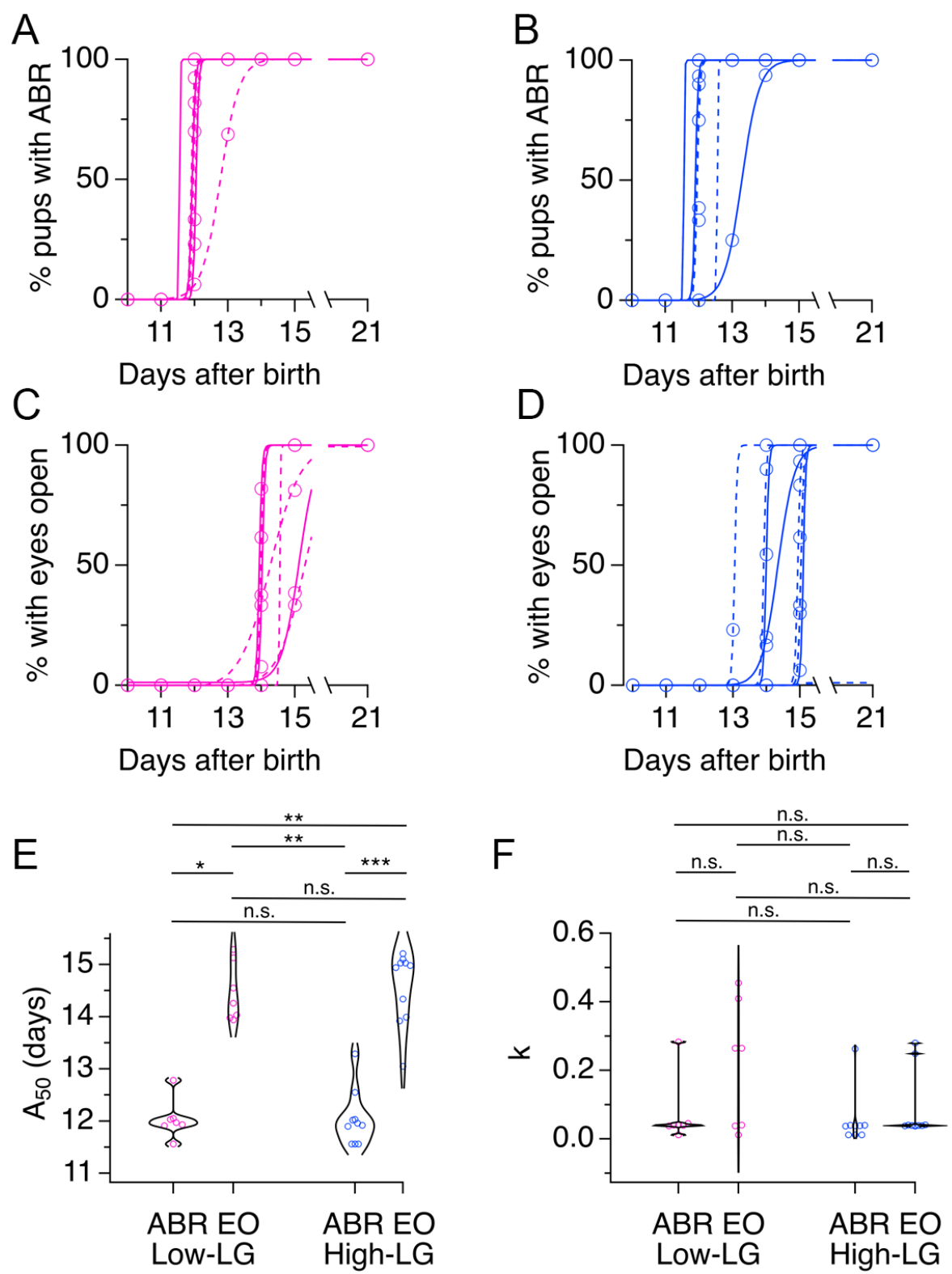
1149 FIGURES AND TABLES
1150
1151 FIGURE 1
1152



1153
1154
1155

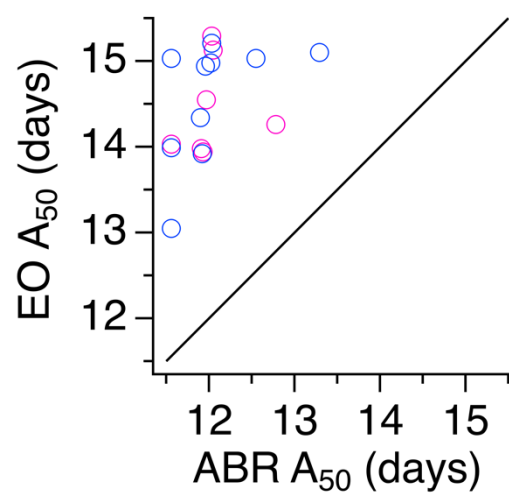


1161 FIGURE 3
1162

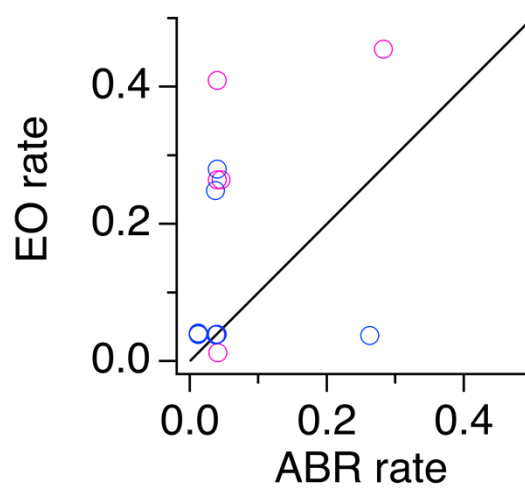


1163
1164 FIGURE 4
1165

A



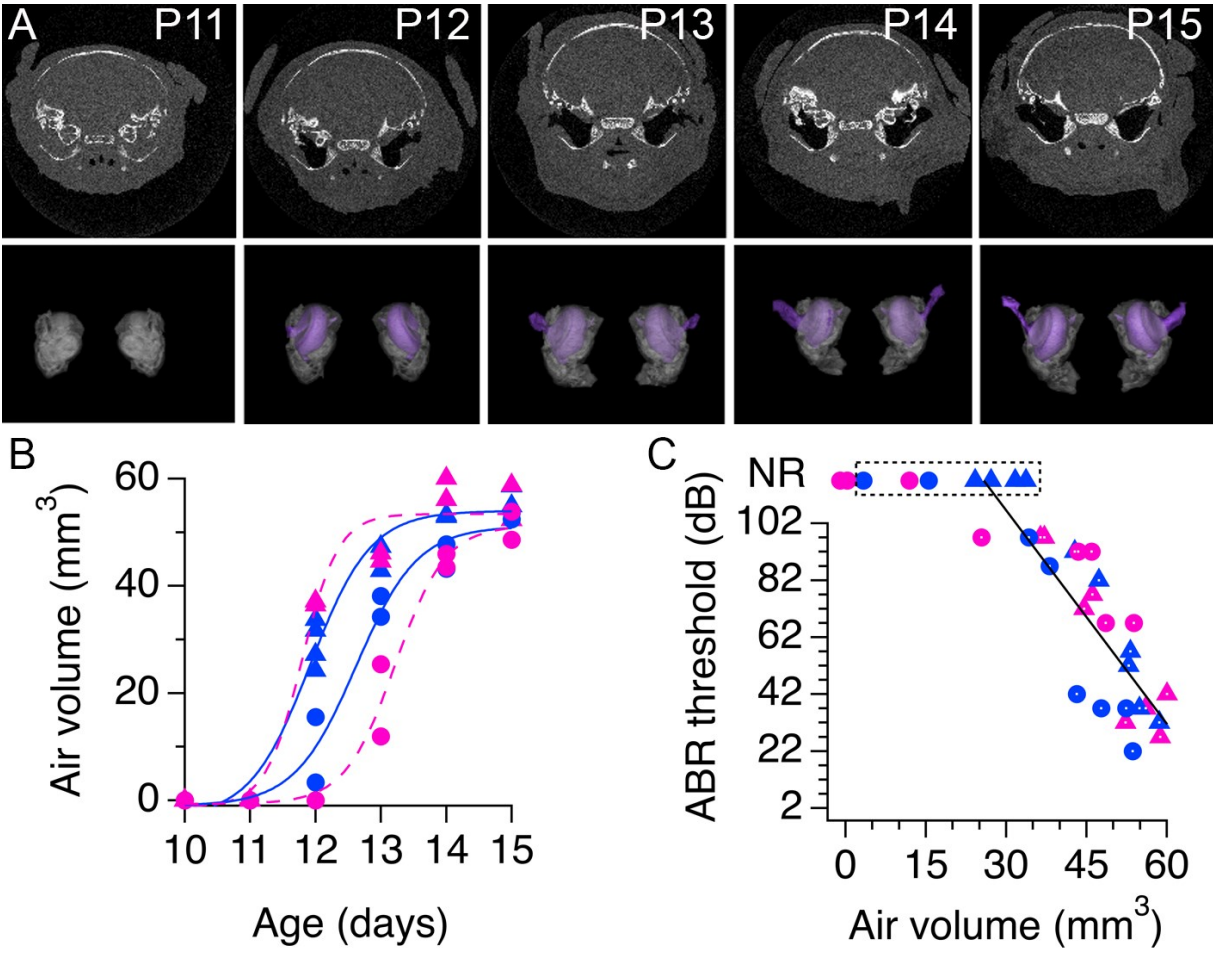
B

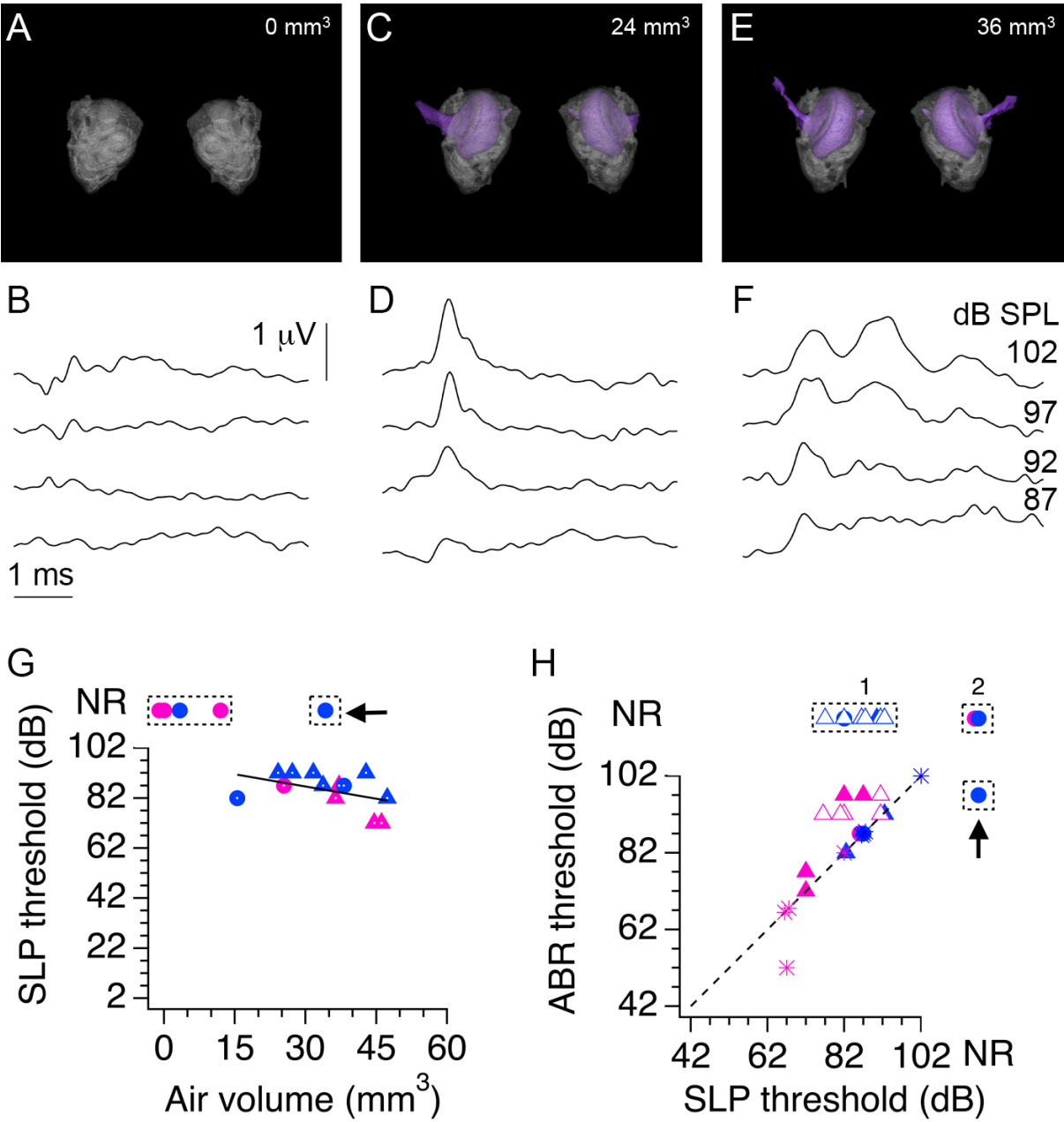


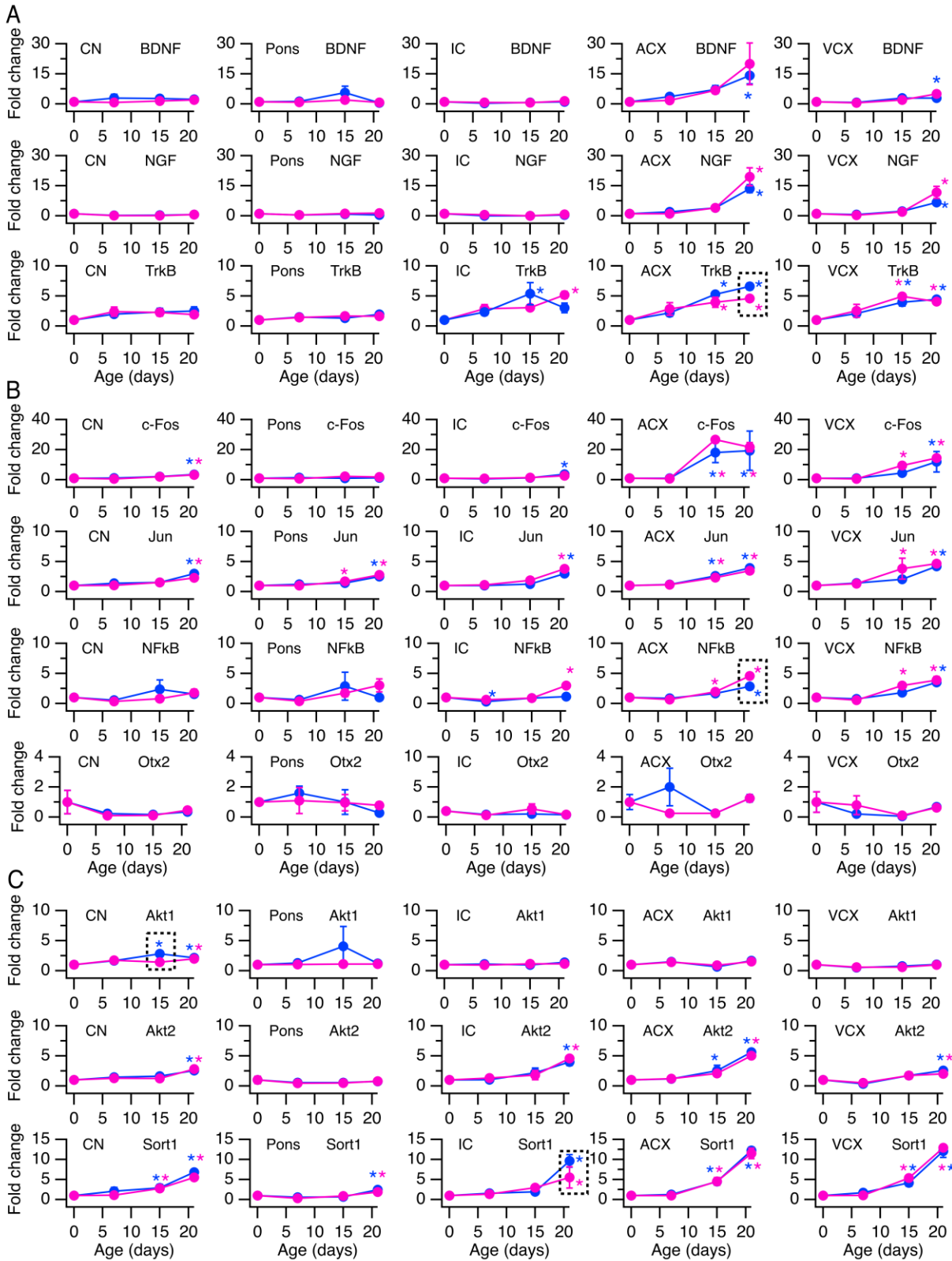
1166

1167

FIGURE 5







1177

1178

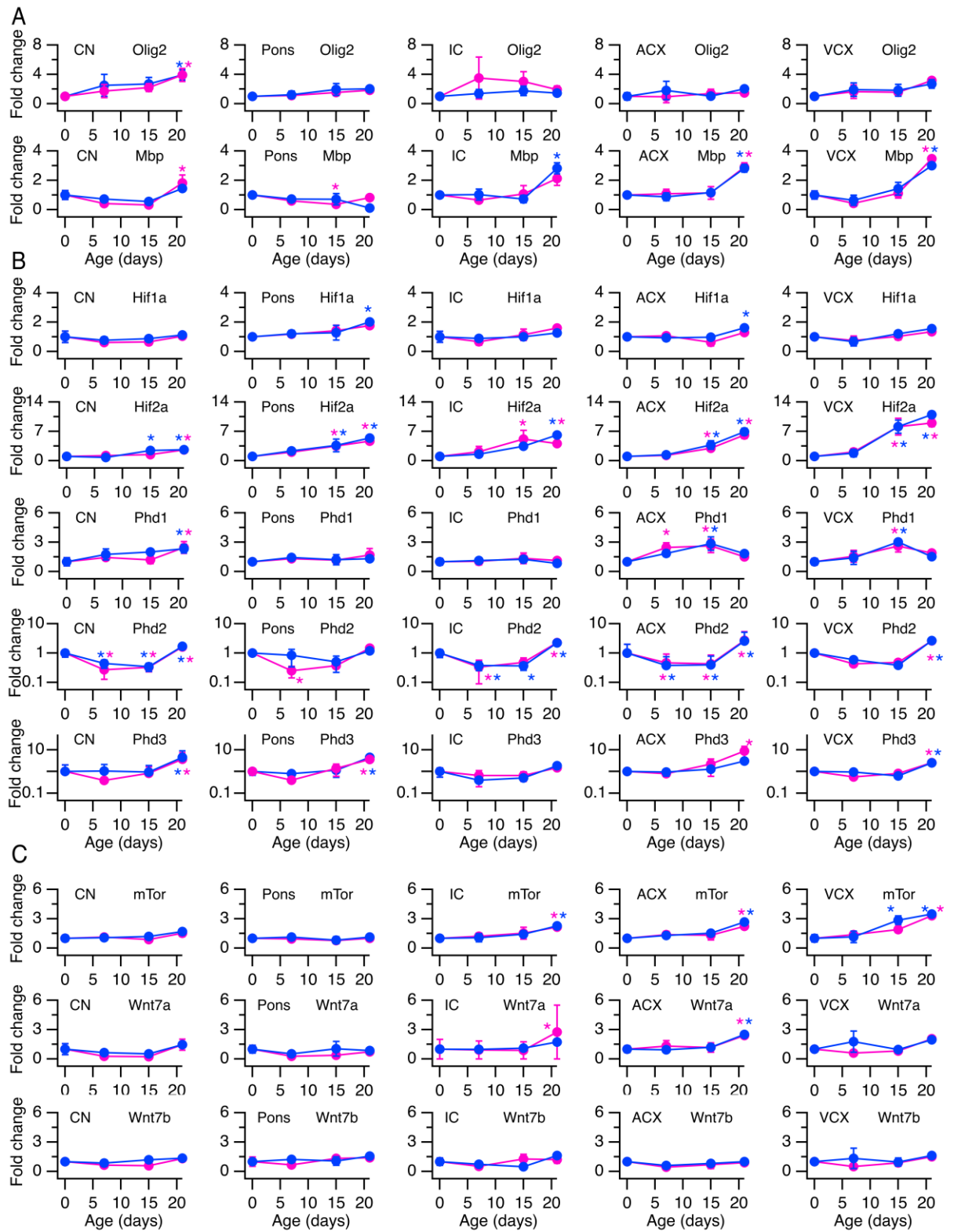
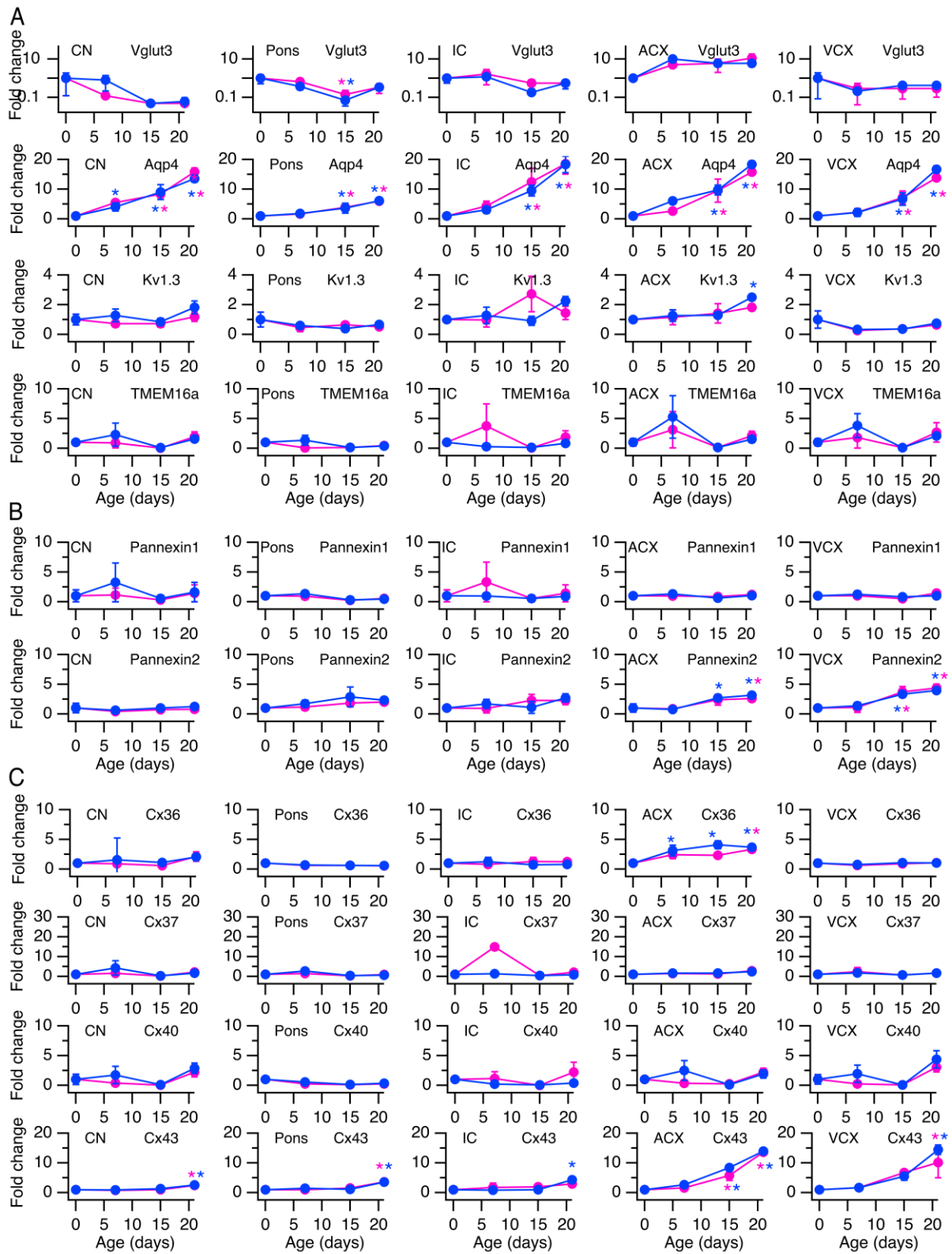


FIGURE 9



1183

1184

1185 TABLE 1. List of primer pairs used for analysis of gene expression with RT-qPCR.
1186

Gene	Gene ID	Sequence (5'-3'); sequence (3'-5')
□-actin	81822	AAGACCTCTATGCCAACAC; TGATCTTCATGGTGCTAGTAGG
Bdnf	24225	GGAGACGAGATTTTAAGACAC; CCATAGTAAGGAAAAGGATGG
Ngf	310738	AAACTAGGCTCCCTGAAG; AGAACAACATGGACATTACG
Trk-B	25054	AATGGAGACTACACCCTAATG; GAGGGGATCTCATTACTTTTG
c-Fos	314322	AAAACCTGGAGTTTATTTTGGC; CACAGACATCTCCTCTGG
c-Jun	24516	AAAAGTGAAAACCTTGAAAGC; CGTGGTTCATGACTTTCTG
NF-κB	81736	AAAAACGAGCCTAGAGATTG; ACATCCTCTTCCTTGTCTTC
Otx2	305858	GAGAGGACTACTTTCACGAG; CGATTCTTAAACCATACCTGC
Akt1	24185	GGGGAATATATTAAACCTGGC; GTCTTCATCAGCTGACATTG
Akt2	25233	GAGTCCTACAGAATACCAGG; AATCTCTGCACCATAAAAGC
Sort1	83576	CTTTACCACCCATGTGAATG; TTTTGAAGGTTTCCCCAAG
Olig2	304103	ATCGAATTCACATTCGGAAG; GAAAAAGATCATCGGGTTCTG
Mbp	24547	GAGAATTAGCATCTGAGAAGG; AAACACATCACTGTCTTCTG
Hif1a	29560	GAAAGGATTACTGAGTTGATGG; CAGACATATCCACCTCTTTTGG
Hif2a	29452	GATGACAGAATCTTGGAAGT; CACACATATCCTCCATGTTTG
Phd1	308457	AAACTCAATTTTCATGAGCAGG; CTGAGGTGTTGAACAGAAAC
Phd2	308913	GAATCAGAACTGGGATGTAAAG; TTGGCATCAAATACCAGAC
Phd3	54702	TGGGGATCCTAATTATCCAG; TCCTGTCCCTCTCATTTAAC
mTor	56718	AGAAATTTGATCAGGTGTGC; TTCCTTTTCCTTCTTGACAC
Wnt7a	114850	ATCATCGTCATAGGAGAAGG; ATAATTGCATAGGTGAAGGC
Wnt7b	315196	CATGAACCTTCACAACAATG; TTGTACTTCTCCTTGAGTAGG
Vglut3	266767	CCTGTCTATGCCATTATTGTG; AGAGACCCACCTTACTTATTG
Aqp4	25293	GAAAACCACTGGATATATTGGG; CAGAAGACATACTCGTAAAGTG

Kv1.3	29731	AACTTCAATTACTTCTACCACC; ACTTACTCAGAGTGGAGTTAC
Tmem16a	309135	GAAATCCTGAAGAGAACAACG; TTTACTTAGAAGGGCAGAGTC
Pannexin1	315435	CTTGACAAAGTCTATAACCGC; ATTAGGTGACTGGAGTTCTTC
Pannexin2	362979	AAACAGCAAGACTGAGAAG; TATAGGGATGCACATCCAAG
Connexin-36	50564	AAATTTGTGACCCATCTCAG; AAAGTGTGTTAGGGCTAATG
Connexin-37	25655	AATTTGACCACCGAGGAG; CATACTGCTTCTTGGATGC
Connexin-40	50563	GTGTATATGTGTGTGTGTGC; AGGGCTCTTCTTTACCATTC
Connexin-43	24392	AAAACGTCTGCTATGACAAG; CACAGACACGAATATGATCTG

1187

1188